



Supplementary Materials for

Tudor-SN-mediated endonucleolytic decay of human-cell microRNAs promotes G1-to-S phase transition

Reyad A. Elbarbary, Keita Miyoshi, Jason R. Myers, Peicheng Du, John M. Ashton, Bin Tian, Lynne E. Maquat*

*Corresponding author. Email: lynne_maquat@urmc.rochester.edu ([L.E.M.](#))

This PDF file includes:

Materials and Methods
figs. S1 to S22
Tables S1 to S8
References (21-35)

Materials and Methods

Plasmid constructions

pCMV-3F-TSN (a gift from K. Nishikura), which we call pCMV-3×FLAG-TSN to be consistent with our pCMV-3×FLAG control, i.e. p3×FLAG-CMV-10 (Sigma), has been described (3). pET28a-TSN(1-863) (previously called pET28c-TSN(22-863) and pET28c-TSN90(114-885) (both gifts from H.S. Yuan) have also been described (21), and pcDNA3-3×FLAG-AGO2 (a gift from H. Siomi) is unpublished.

The domain structure of TSN was assessed using the Pfam database (<http://pfam.xfam.org/>). To construct pET28a-TSN(1-885), which produces HIS-TSN(WT), a 1.9-kbp fragment was excised from the 3' end of pET28c-TSN90(114-885) (21) using SacI and ligated to SacI-digested pET28a-TSN(1-863) (previously called pET28c-TSN(22-863) (21).

To construct pCMV-3×FLAG-TSN^R, which encodes TSN siRNA-resistant FLAG-TSN, overlap-extension PCR was used. The 5' fragment of TSN was amplified using 5'-AAGCAGAGCTCGTTT~~AGTGAACCG~~-3' (sense) and 5'-~~GTTGTTCGCGGC~~~~CATTC~~~~CCTCTCTCCGGGTGGCTA~~-3' (antisense, where here and elsewhere bold italicized nucleotides confer siRNA-resistance, denoted as “^R”), and the 3' fragment was amplified using 5'-~~AGGGAATGCGCGCAACAACCCTGAGCAGAACCGG~~-3' (sense) and 5'-~~CAGGAGGAGCTCTGTGATGTTGCC~~-3' (antisense). The resulting fragments were mixed and amplified using the same sense and antisense primers that amplified, respectively, the 5' and 3' fragments. The resulting PCR product was then cleaved with SacI and ligated into SacI-digested pCMV-3×FLAG-TSN.

pET28a-TSNΔSN2(Δ164-306), pET28a-TSNΔSN3(Δ312-467), and pET28a-TSNΔSN4(Δ500-635) were constructed as described for pCMV-3×FLAG-TSN^R. Template plasmids and primers used to amplify the 5' and 3' fragments, and the restriction enzymes used to digest PCR products and plasmids, are listed (Table S6).

To construct pET28a-TSNΔSN1(142-885), a PCR-amplified fragment was generated using pET28a-TSN(1-885) and the primer-pair 5'-~~CATGGATCCGGGAACGGTTCACATACTATC~~-3' (sense, where underlined nucleotides specify a BamHI site) and 5'-GTGCTCGAGTGC~~GGCCGCAAGCTTG~~-3' (antisense). The resulting PCR product was digested using BamHI and EcoRI, and ligated to BamHI- and EcoRI-digested pET28a-TSN(1-885).

To construct pET28a-TSNΔSN5(1-783), a PCR-amplified fragment was generated using pET28a-TSN(1-885) and the primer-pair 5'-~~ACATGTTTGAGGCCCGGAATTTCTTCGAA~~-3' (sense) and 5'-~~CGCAAGCTTCTAATCATCATCTTGGGGCAC~~-3' (antisense, where underlined nucleotides specify a HindIII site). The resulting PCR product was digested using HindIII and ligated to HindIII-digested pET28a-TSN(1-885).

To construct pET28a-EGFP, EGFP cDNA sequences were PCR-amplified from pEGFP-N1 (Clontech) using the primer-pair 5'-~~GAACATATGGTGAGCAAGGGCGAGGAG~~-3' (sense, where underlined nucleotides specify a NdeI site) and 5'-~~CGCGAATTCTTACTTGTACAGCTCGTC~~-3' (antisense, where underlined nucleotides specify an EcoRI site). The resulting PCR product was digested using NdeI and EcoRI, and inserted into NdeI and EcoRI sites of pET28a.

To construct pcDNA3-3×FLAG-AGO2^R, the expression of which is resistant to AGO2 siRNA, overlap-extension PCR was used. A 5′ sequence of AGO2 cDNA was PCR-amplified using pcDNA3-3×FLAG-AGO2 as a template DNA, 5′-CAAGGAATTCATGTACTCGGGAGCC-3′ (sense) and 5′-TTTATGCAGCGCTGGCCGGCCACAATGTTACAGAC-3′ (antisense), and a 3′ sequence was PCR-amplified using 5′-GCCGGCCAGCGCTGCATAAAAAATTAACGGACAATC-3′ (sense) and 5′-GCAGAATTCTCAAGCAAAGTACATGGTG-3′ (antisense). The resulting fragments were mixed and amplified using the same sense and antisense primers that amplified, respectively, the 5′ and 3′ sequences. The resulting PCR product was then cleaved with EcoRI and ligated into EcoRI-digested pcDNA3-3×FLAG-AGO2.

Note that the remaining TSN- and AGO2-expressing plasmids are siRNA-resistant even though they will be referred to in the manuscript without such designation unless relevant to the experiment. To construct pCMV-3×FLAG-TSN^RΔSN1(142-885), a PCR-amplified fragment was generated using pCMV-3×FLAG-TSN^R and the primer-pair 5′-CATCCGCGGGGAACGGTTCACATACTATC-3′ (sense) and 5′-CATCCGCGGGGAACGGTTCACATACTATC-3′ (antisense). The resulting PCR product was digested using SacI and NheI, and ligated to SacI- and NheI-digested pCMV-3×FLAG-TSN^R.

To construct pCMV-3×FLAG-TSN^RΔSN4(Δ500-635), a 1.2-kbp fragment was excised from pET28a-TSNΔSN4(Δ500-635) using BstZ17I and NheI and ligated to BstZ17I- and NheI-digested pCMV-3×FLAG-TSN^R.

To construct the retroviral expression vector pLHCX-3×FLAG-AGO2^R, the entire 3×FLAG-AGO2^R coding region was excised from pcDNA3-3×FLAG-AGO2^R using HindIII and XbaI. The HindIII- and XbaI-generated ends were made blunt using Quick blunting kit (BioLabs), and the resulting blunt-ended fragment was inserted into HpaI-digested pLHCX (Clontech).

To construct the retroviral expression vector pLHCX-3×FLAG, the synthetic DNA duplex of 5′-ATGGACTACAAAGACCATGACGGTGATTATAAAGATCATGACATCGATTACAAGGATGACGATGACTAA-3′ and 5′-TTAGTCATCGTCATCCTTGTAATCGATGTCATGATCTTTATAATCACCGTCATGTCTTTGTAGTCCAT-3′) was inserted into HpaI-digested pLHCX.

To construct the pSpCas9n(BB)-2A-Puro-TSN-sgRNA1, a synthetic DNA duplex of 5′-CACCGAGTTGATCTGCCGCTCAGG-3′ and 5′-AAACCCTGAGCGGCAGATCAACCTC-3′ was inserted into BbsI-digested pSpCas9n(BB)-2A-Puro (PX462) (Addgene).

pSpCas9n(BB)-2A-Puro-TSN-sgRNA2, 3 and 4 were constructed as described for pSpCas9n(BB)-2A-Puro-TSN-sgRNA1. Synthetic DNA duplexes are listed (Table S7).

To construct the lentiviral expression vector pLVX-Puro-3×FLAG-TSN(910), where 910 indicates that the full-length 910-amino acid protein is encoded, the TSN coding region and 3′UTR were PCR-amplified using the plasmid HsCD00323421 (Harvard Medical School) and the primer-pair 5′-TATGCGGCCGCGGCGTCCTCCGCGCAGAGC-3′ (sense, where underlined nucleotides specify a NotI site) and 5′-

CTAGGATCCGCAGACAGCACGTACTATTTTATTG-3' (antisense, where underlined nucleotides specify a BamHI site). The resulting PCR product was digested using NotI and BamHI and ligated to NotI- and BamHI-digested pCMV-3×FLAG-TSN(910)+3'UTR plasmid. The resulting plasmid was used to PCR-amplify the entire 3×FLAG-TSN(910)+3'UTR sequence using the primer-pair 5'-AGCGTTAACATGGACTACAAAGACCATGACGG-3' (sense, where underlined nucleotides specify a HpaI site) and 5'-CTAGGATCCGCAGACAGCACGTACTATTTTATTG -3' (antisense, where underlined nucleotides specify a BamHI site). The resulting PCR product was digested using HpaI and BamHI and ligated to SmaI and BamHI-digested pLVX-Puro vector (Clontech).

To construct the retroviral expression vector pLVX-Puro-3×FLAG, 5'-ATGGACTACAAAGACCATGACGGTGATTATAAAGATCATGACATCGATTACAAGGATGACGATGACTAA-3' and 5'-TTAGTCATCGTCATCCTTGTAATCGATGTCATGATCTTTATAATCACCGTCATGTCTTTGTAGTCCAT-3' were annealed and inserted into SmaI-digested pLVX-Puro vector (Clontech).

Cell culture and transfections

Human HEK293T (ATCC), Dicer-kd 2b2 (a gift from P. Svoboda) (20) and HeLa (ATCC) cells were propagated in Dulbecco's Modified Eagle's Medium (Gibco) supplemented with 10% fetal bovine serum (Seradigm). HEK293T cells were transiently transfected with plasmid DNA using Lipofectamine 2000 (Invitrogen). Where specified, HEK293T or HeLa cells were transfected with siRNA (GE Healthcare Dharmacon), a miRNA mimic, or a miRNA inhibitor (Qiagen) using RNAiMAX (Invitrogen), or were incubated with 200 μM pdTp (Carbosynth). To induce Dicer shRNA expression, Dicer-kd 2b2 cells were cultured in medium containing 1 μg/mL of doxycycline hydrochloride (Sigma). Stable HEK293T-cell transfectants were generated using pLHCX-3×FLAG or pLHCX-3×FLAG-AGO2^R as described (22). Notably, superscript "R", indicating siRNA-resistance, is omitted from figures and text when not relevant to experiments.

TSN knockout HEK293T cell lines (TSN KO#1 and TSN KO#2) were established using the double-nicking strategy, i.e. the D10A mutant Cas9 nickase (Cas9n) and two small guide RNAs (sgRNAs), to minimize off-target effects (14). TSN KO#1 was generated with TSN-sgRNA1 and TSN-sgRNA2, and TSN KO#2 was generated with TSN-sgRNA3 and TSN-sgRNA4. sgRNAs target sites were selected using CRISPR Design Tool (<http://www.genome-engineering.org/crispr/>) (14).

TSN KO#1 cells the stably express 3×FLAG or 3×FLAG-TSN(910) were generated using pLVX-Puro-3×FLAG-TSN(910) or pLVX-Puro-3×FLAG as described (22).

siRNAs

TSN siRNA consisted of 5'-GAUUAUUAGCUCUCAUGCCdTdT-3', and AGO2 siRNA, to which FLAG-AGO2 mRNA expressed from the pcDNA3-3×FLAG-AGO2^R plasmid is resistant, was 5'-UAAUACAUCUUUGUCCUGCdTdT-3' (GE Healthcare Dharmacon). Control siRNA was Silencer Negative Control #1 siRNA (Thermo Fisher Scientific).

Western blotting

Cells were lysed in RIPA Buffer, and total-cell proteins were separated in a 6-15% denaturing polyacrylamide gel, transferred to nitrocellulose (Amersham Biosciences), and probed using antibodies recognizing TSN (Abcam), GAPDH (Santa Cruz), Calnexin (Enzo Life Sciences), ITGA5 (Abcam), LOX (Novus Biologicals), Dicer (Abcam), AGO2 (Abcam), GW182 (Bethyl Laboratories), PABPC1 (Santa Cruz Biotechnologies), FLAG (Sigma), CDK2 (Abcam), CCND1 (Abcam), E2F1 (Abcam), or E2F2 (Abcam). Blots were quantified using Image Quant (Molecular Dynamics).

Immunoprecipitations

Cells were crosslinked using 0.2% formaldehyde (Sigma) prior to lysis, and lysate proteins and/or RNAs were analyzed before and after immunoprecipitation (IP) as reported (23) with slight modifications: cells were lysed, and IPs were performed in lysis buffer [20 mM HEPES pH 7.4, 300 mM NaCl, 2 mM MgCl₂, 2 mM CaCl₂, 1 mM dithiothreitol (DTT), 0.5 % NP-40, and cOmplete Mini, EDTA-free Protease Inhibitor Cocktail Tablets (Roche)]. When indicated, RNase I (1 U/μl, Promega) was used for RNA digestion as described (24). FLAG IPs were performed using anti-FLAG M2 Agarose Affinity Gel (Sigma). TSN IPs were performed using Dynabeads Protein A (Life Technologies) conjugated to polyclonal anti-TSN (Abcam) or, as a control, rabbit IgG (Thermo Fisher Scientific).

RNA purification, RT-qPCR and Northern blotting

RNA fractions enriched in < 200-nt RNAs were purified from cell pellets using miRNeasy and RNeasy MinElute Cleanup Kits (Qiagen) for analyses of miRNAs and pre-miRNAs. The corresponding fractions that contained > 200-nt RNAs were used to quantitate pri-miRNAs and mRNAs. For quantitation of miRNAs and pre-miRNAs, cDNAs were prepared using miScript II RT Kit (Qiagen) and subsequently qPCR-amplified using miScript Primer Assay kits (Qiagen) for miRNAs or miScript Precursor Assay kits (Qiagen) for pre-miRNAs. qPCR was performed using miScript SYBR Green PCR kits (Qiagen) and the 7500 Fast Real-Time PCR System (Applied Biosystems). Although the stem-loop sequences targeted by the miScript Precursor Assay are present in both pri- and pre-miRNAs, the fraction of < 200-nt RNAs used to quantitate pre-miRNAs was completely devoid of pri-miRNAs (see below for the method used to specifically quantitate pri-miRNAs). Notably, when a primer set was first used, identity of the resulting PCR product was confirmed by cloning and sequencing. Once confirmed, melting curves were used in each subsequent PCR to verify that each primer set reproducibly and specifically generates the same PCR product. Results of miScript Primer Assay Kits (Qiagen) in Fig. 1 were confirmed using miRCURY LNA Universal RT microRNA PCR (Exiqon). Normalizing the levels of miRNAs and pre-miRNAs to the level of U61 snoRNA gave comparable results to those in Fig. 1, where the levels of miRNAs and pre-miRNAs were normalized to U6 snRNA. For quantitation of pri-miRNAs and, in Fig. 4C and fig. S22, mRNAs, cDNAs were prepared using iScript Reverse Transcription Supermix for RT-qPCR (Bio-Rad). cDNAs were qPCR-amplified using TaqMan Pri-miRNA Assay (Thermo Fisher Scientific) for pri-miRNAs quantitation, and TaqMan Gene Expression Assay (Thermo Fisher Scientific) for mRNAs quantitation. To quantitate TSN and GAPDH mRNAs (fig. S19), cDNAs were prepared

using SuperScript III reverse transcriptase (Invitrogen) and subsequently qPCR-amplified using primer pairs specified in Table S8 and Fast SYBR Green Master Mix (Applied Biosystems). *P*-values were calculated using the two-tailed Student's *t*-test.

Northern blotting for miRNA was performed essentially as previously described (25). RNA fractions that were enriched in < 200-nt RNAs (equivalent to 30 µg of total RNA) were electrophoresed in 12% acrylamide denaturing urea gels and then transferred using electroblotting to Hybond N+ membranes (GE Healthcare). After transfer, they were UV-crosslinked and baked for 1 h at 80°C. DNA and locked nucleic acid (LNA) probes were labeled with T4 polynucleotide kinase (NEB) and [γ -³²P]ATP (Perkinelmer) and hybridized to the membranes at 42°C in 7% SDS, 1 mM EDTA, and 200 mM Na₂PO₄ (pH 7.4) overnight. Membranes were washed twice with 2× SSC, 0.1% SDS. The blots were exposed using a Typhoon Phosphorimager 9410 (GE Biosciences). Different DNA and LNA probes were tested, and the following proved to be the most efficient and, thus, were used for detection: DNA probe 5'-AGCTATGCCAGCATCTTGCCT-3' for miR-31-5p; DNA probe 5'-TCACAGGTTAAAGGGTCTCAGGGA-3' for miR-125a-5p; DNA probe 5'-CGCATTATTACTCACGGTACGA-3' for miR-126-3p; DNA probe 5'-AGAATCCTTGCCCGGGTGCATTGCATTTCAGAAAGCAC-3', which spans mature miR-501-3p and the loop region of pre-miR-501; DNA probe 5'-CACCTTTTCAAATCCACAAACCATTATGTGCTGCTA-3, which spans mature miR-15a-5p and the loop region of pre-miR-15a; DNA probe 5'-TGTTTAATATATATTTCACTACGCCAATATTTACGTGCTGCTA-3', which spans mature miR-16-5p and the loop region of pre-miR-16; DNA probe 5'-GCAGGGGCCATGCTAATCTTCTCTGTATCG-3' for U6 snRNA. miRCURY LNA Detection probe (Exiqon, 610990-300) was used for miR-29b-3p.

Purification of recombinant proteins

HIS-tagged TSN variants and HIS-tagged EGFP were expressed in BL21-*CodonPlus(DE3)*-RIPL cells (Agilent Technologies), purified on a HisTrap HP column (GE Healthcare), and further purified on a HiTrap Q HP column (GE Healthcare) as described (26, 27). Concentrations of recombinant proteins were estimated after electrophoresis in SDS-polyacrylamide gels using Coomassie Blue (Sigma), where serial dilutions of bovine serum albumin (Rockland) provided concentration standards.

Preparing and sequencing small RNA libraries

Run #1: The TruSeq Small RNA library preparation protocol (Illumina) was employed to generate cDNA libraries using small RNA fractions (< 200 nucleotides) derived from HEK293T-cell lines. After addition of the TruSeq 3' adapter (5' adenylated) using truncated T4 RNA ligase II (New England Biolabs) and, subsequently, the 5' adapter using T4 RNA ligase I (New England Biolabs), RNA was reverse-transcribed using a 3' adapter-specific primer. The resulting cDNA was then amplified using 12 cycles of PCR, a universal forward primer and a reverse primer, the latter harboring a bar code. cDNA libraries were purified from 8% polyacrylamide and quantitated first using an Agilent Bioanalyzer and subsequently using qPCR. Barcoded libraries were mixed at equimolar concentrations and sequenced using a NextSeq 500 machine (Illumina). All steps were performed at the Rutgers-New Jersey Medical School Genomics Core.

Run #2: cDNA libraries were prepared using total HEK293T-cell RNA as described for Run #1. After addition of the TruSeq 3' adapter (5' adenylated) using truncated T4 RNA ligase II (New England Biolabs) and, subsequently, the 5' adapter using T4 RNA ligase I (New England Biolabs), RNA was reverse-transcribed using a 3' adapter-specific primer. The resulting cDNA was then amplified using 12 cycles of PCR, a universal forward primer and a reverse primer, the latter harboring a bar code. cDNA libraries were purified using the Pippin Prep (Sage Science) and quantified as described for Run #1. Barcoded libraries were mixed at equimolar concentrations and sequenced using a HiSeq2500v4 sequencer (Illumina) by single-end 50-nt sequencing. All steps were performed at the University of Rochester Genomics Research Center.

Computational analyses of for Runs #1 and #2 miR-seq data

For reads in each Run, subsequences that reside between the 5' and 3' Illumina adapters were extracted as inserts. For Run #1, the four nucleotides on either side of the inserts that derived from random priming were trimmed using an in-house Perl script. Inserts that consisted of 18- 25 nucleotides in either Run were then selected as potential miRNA sequences using the same Perl script. For Run #2, reads were trimmed using cutadapt v1.12 and the command line options of “-m 18 -M 25 -q 10 -e 0.12”. Sequences were mapped to the human mature miRNA database (miRBase, Release 21) using BOWTIE2 (28) v2.2.5 and default parameters. Mapped reads were counted using SAMtools (29) v0.1.12a and default parameters. The DESeq2 package (30) v1.4.5 of R v3.1.1 was used to normalize counts, perform differential expression analyses, and adjust *P*-values for multiple testing using the Benjamini-Hochberg procedure and default options of the results() command. The significance level of the adjusted *P*-value was 0.05. Heat maps were produced using the pHeatmap v1.0.8 package (31) with row scaling and hierarchical clustering of the rLog-transformed expression values after removing batch effects using the removeBatchEffect() command from the Limma v3.30.12 package (32). Pair-wise correlations between samples shown in Fig. S10 were derived using the rLog-transformed expression values for every gene as input to the cor() function of the stats package (33) and ‘method=spearman’. Batch effects were removed as described above prior to correlation calculations. Correlation values were visualized using the corrplot v0.77 package (34) with ‘method="number", order="hclust"’.

Electrophoretic mobility shift assays (EMSAs)

EMSA was performed as previously described with slight modifications (27). Briefly, 5'-[³²P]-miR-31-5p was incubated with the specified recombinant TSN variant for 1.5 h at 4°C in binding buffer (40 mM Tris-HCl pH 8, 30 mM KCl, 1 mM MgCl₂, 0.01% NP40, and 1 mM DTT). Loading buffer (60 mM KCl, 10 mM Tris-HCl pH 7.6, 5% glycerol, 0.01% xylene cyanol, and 0.01% bromophenol blue) was added, and protein-RNA complexes were electrophoresed in a 15% native polyacrylamide gel at 4°C.

Molecular weight standards used to map miRNA cleavage products

To generate an alkaline hydrolysis ladders for cleavage-site mapping, each 5'-[³²P]-labeled miRNA (10,000 cpm) was mixed with 200 ng of yeast RNA (Thermo Fisher Scientific), and the mixture was incubated with alkaline hydrolysis buffer [50 mM NaHCO₃/Na₂CO₃

pH 9.2, and 1 mM EDTA] for 7.5 min at 95°C. The reaction was stopped by adding Gel Loading Buffer II (Thermo Fisher Scientific).

To generate ladders of G-specific cleavages, each mixture of 5'-[³²P]-labeled miRNAs (10,000 cpm) and 200 ng of yeast RNA was incubated with 0.1 U RNase T1 (Thermo Fisher Scientific) for 5 min at room temperature. Reaction products were recovered by ethanol precipitation.

In vitro nuclease assays

Synthetic single-stranded miRNAs (Integrated DNA Technology) were 5'-end labeled using γ -[³²P]ATP (PerkinElmer) and T4 polynucleotide kinase (New England Biolabs) or 3'-end labeled using [5'-³²P]Cp (cytidine 3', 5'-bisphosphate) (PerkinElmer) and T4 RNA ligase (Thermo Fisher Scientific). For nuclease assays, labeled miRNAs (100-200 fmol) were incubated for 2 h at 37 °C (unless otherwise indicated) with *E. coli*-produced HIS-TSN or HIS-EGFP (1-2 pmol) in 15 μ l of Nuclease Reaction Buffer [50 mM HEPES-KOH pH 7.5, 5 mM CaCl₂, 100 mM NaCl, and 1 mM ATP]. Reactions were terminated by adding 1 μ l of proteinase K (Thermo Fisher Scientific) for 5 min at 37°C, and products were purified using RNeasy MinElute Cleanup Kits (Qiagen) or directly boiled in Gel Loading Buffer II (Thermo Fisher Scientific), electrophoresed in 6M urea-15% polyacrylamide, and visualized using a Typhoon Phosphorimager 9410 (GE Biosciences).

Assembly of 5'-[³²P]-miR-31-5p into AGO2 complexes

HEK293T cells stably expressing 3 \times FLAG-AGO2 were lysed using a Dounce homogenizer in Lysis Buffer [30 mM HEPES-KOH pH 7.4, 100 mM potassium acetate, 2 mM magnesium acetate, and 5 mM DTT]. Lysates were incubated for 1 h at 37°C with 5'-[³²P]-miR-31-5p : 5'-[P]-miR-31-3p duplex in Loading Buffer [15 mM HEPES-KOH pH 7.4, 54 mM potassium acetate, 1 mM magnesium acetate, 8.5 mM DTT, 30 mM creatine phosphate, 0.4 U/ μ l RNaseOUT (Thermo Fisher Scientific), 1.2 mM ATP, 0.3 mM GTP, and 90 μ g/ml creatine kinase]. NaCl was then added to a final concentration of 150 mM, and 3 \times FLAG-AGO2 was immunoprecipitated. Washing was performed using Washing Buffer [50 mM Tris-HCl pH 7.4, 150 mM NaCl, and 0.05% NP40], and the final wash was confirmed to be free of radioactivity. Anti-FLAG IPs were spiked with *in vitro*-synthesized, internally [³²P]-labeled RNA before RNA extraction.

Assays for degradation of AGO2-bound miRNA by HIS-TSN, RNase I or Exo T

Assays were performed as described in the previous section except that beads were further washed with Nuclease Reaction Buffer, and incubated for 2 h with 50 μ l of Nuclease Reaction Buffer that did not (“-” sample in Fig. 3E) or did contain either 5 pmol of HIS-TSN or 10 U of RNase I (Promega), each at 37°C, or 10 U of Exo T (New England Biolabs) at 25°C. It is of note that each amount of added nuclease consists of a comparable amount of protein (Coomassie blue staining) and comparable degradative activity. Samples were then incubated for 5 min at 37°C with 5 μ l of proteinase K (Thermo Fisher Scientific). RNA was extracted from samples (beads + supernatant) using RNeasy MinElute Cleanup Kits (Qiagen) and electrophoresed in 6M urea-15% polyacrylamide. Importantly, we did not detect radioactivity in the supernatant of “-”

samples, confirming that the complex of AGO2 with 5' -[³²P]-miR-31-5p did not non-specifically dissociate during incubation.

Cell synchronization and flow cytometry

HEK293T cells were synchronized at G1/S using a double-thymidine block as previously reported (35). Briefly, cells were incubated in culture medium that contains 2 mM thymidine (Sigma) for 17 h, washed and incubated in fresh medium for 8 h, and incubated again in culture medium that contains 2 mM thymidine for 15 h. Cells were then washed and incubated in fresh medium until harvest time.

For synchronization in prometaphase, HEK293T cells were incubated in culture medium that contains 50 ng/ml nocodazole (Sigma) for 16 h. Cells were then washed and incubated in fresh medium until harvest time.

Harvested samples were suspended in phosphate-buffered saline (PBS), and fixed in 70% ethanol for 2 h on ice. Prior to flow cytometric analyses, samples were incubated overnight on ice protected from light in 50 µg/ml propidium iodide (Life Technologies), 0.2 mg/ml RNase A (Sigma), and 0.1% Triton X-100 in PBS. Flow cytometry was performed using a LSRII flow cytometer (BD Biosciences) with FACSDiva software. Cell-cycle modeling was performed using Flowjo software. For each sample, 50,000 events were collected, and aggregated cells were gated out. Percentages of cells existing within the different phases of the cell cycle were calculated using Flowjo software.

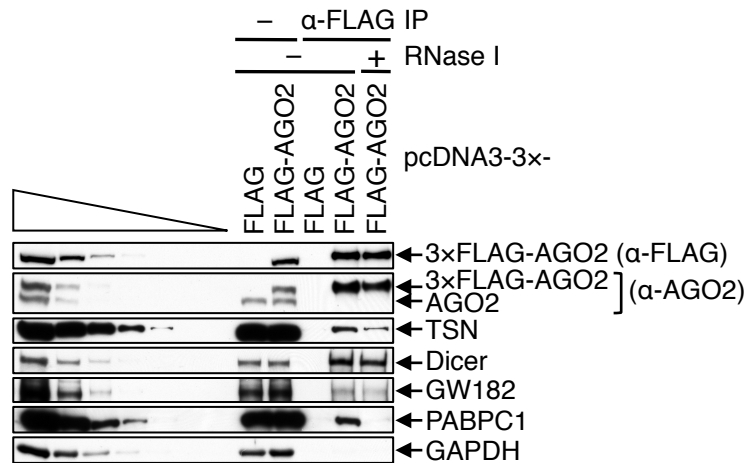


Fig. S1. FLAG-AGO2 co-immunoprecipitates with cellular TSN

Western blot (WB) before (-) or after anti(α)-FLAG IP of 3 \times FLAG-AGO2, which was exogenously expressed in HEK293T cells at essentially the same level of cellular AGO2, or FLAG, as a negative control, demonstrating that 3 \times FLAG-AGO2 co-immunoprecipitates with cellular TSN in the presence (+) or absence (-) of RNase I. Dicer and GW182 serve as positive IP controls. The absence of PABPC1 in the RNase I-treated 3 \times FLAG-AGO2 IP confirms RNase activity, and IP specificity was demonstrated by the absence of GAPDH in all IPs. Here and elsewhere, the leftmost lanes under the wedge analyzed 3-fold dilutions of lysate. Results are representative of 3 independently performed experiments.

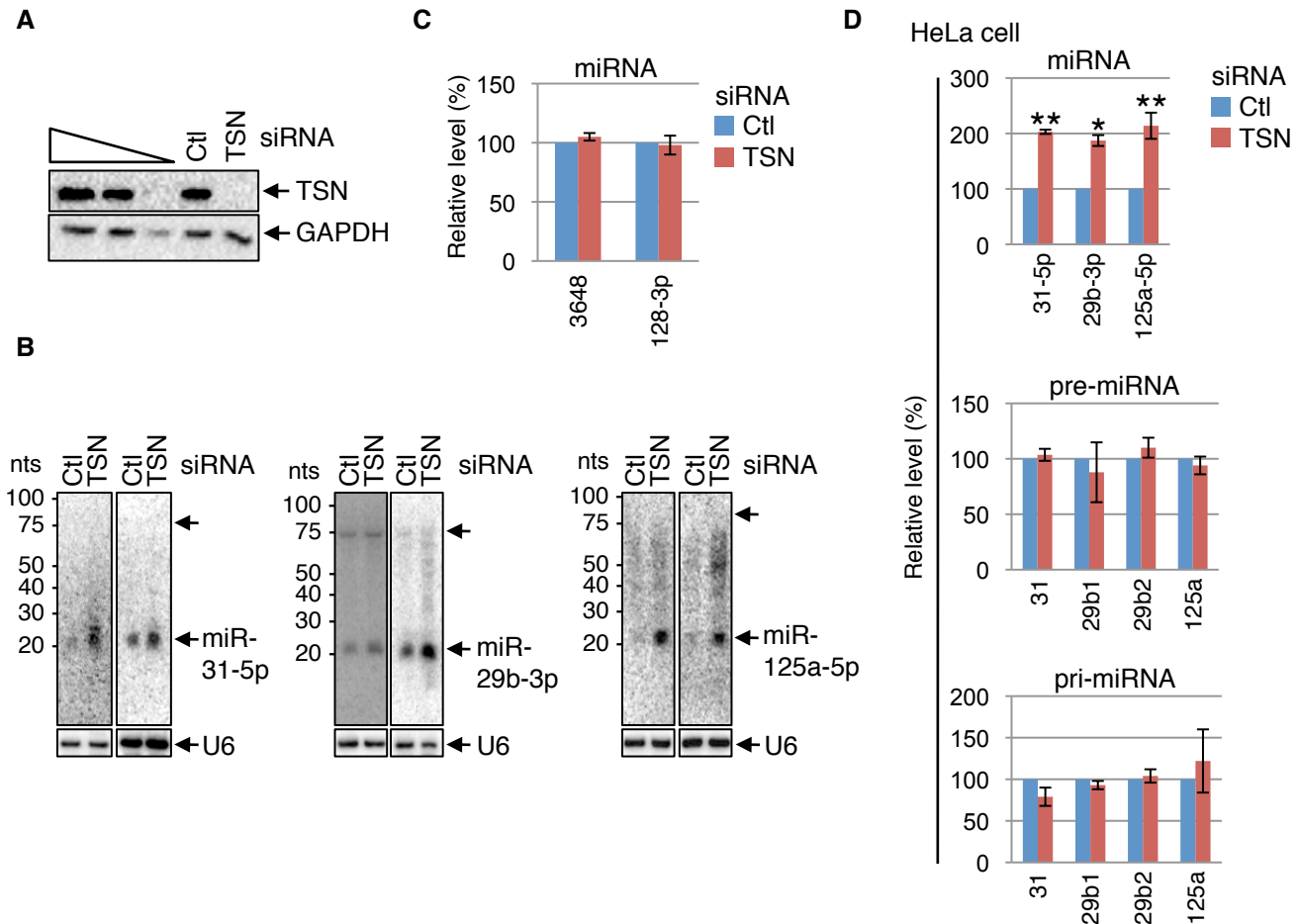


Fig. S2. TumiD typifies not only HEK293T cells but also HeLa cells

(A) WB demonstrating downregulation of TSN expression in TSN siRNA-transfected HEK293T cells compared to Control (Ctl) siRNA-transfected cells. GAPDH serves as a loading control. (B) Northern blotting from two representative blots showing that the levels of mature miRNAs increased in cells transfected with TSN siRNA relative to Ctl siRNA, while the levels of pre-miR-29b did not significantly change. Arrowheads specify the positions where pre-miRs are expected to migrate and illustrate that pre-miR-31 and pre-miR-125a were not detectable here, as was also true for other ≥ 4 repeated attempts. (C) Histogram representations of RT-qPCR results showing that the levels of miR-3648 and miR-128-3p remain unchanged in TSN siRNA-transfected HEK293T cells relative to Ctl siRNA-transfected cells. The level of each miRNA is relative to the level of U6 snRNA, and relative levels in Ctl siRNA-transfected cells are defined as 100. (D) Histogram representations of RT-qPCR results demonstrating that the levels of mature miRNAs shown to be TumiD targets in HEK293T cells (Fig. 1B) are increased upon TSN knockdown in HeLa cells, while the levels of their corresponding pre- and pri-miRNAs remain unchanged. miRNAs and pre-miRNAs levels are relative to the level of U6 snRNA, pri-miRNA levels are relative to the level of β -actin mRNA, and relative levels in the presence of Ctl siRNA are defined as 100. All results derive from ≥ 3 independent experiments. Histograms represent the average and SD. * $P < 0.05$, ** $P < 0.01$.

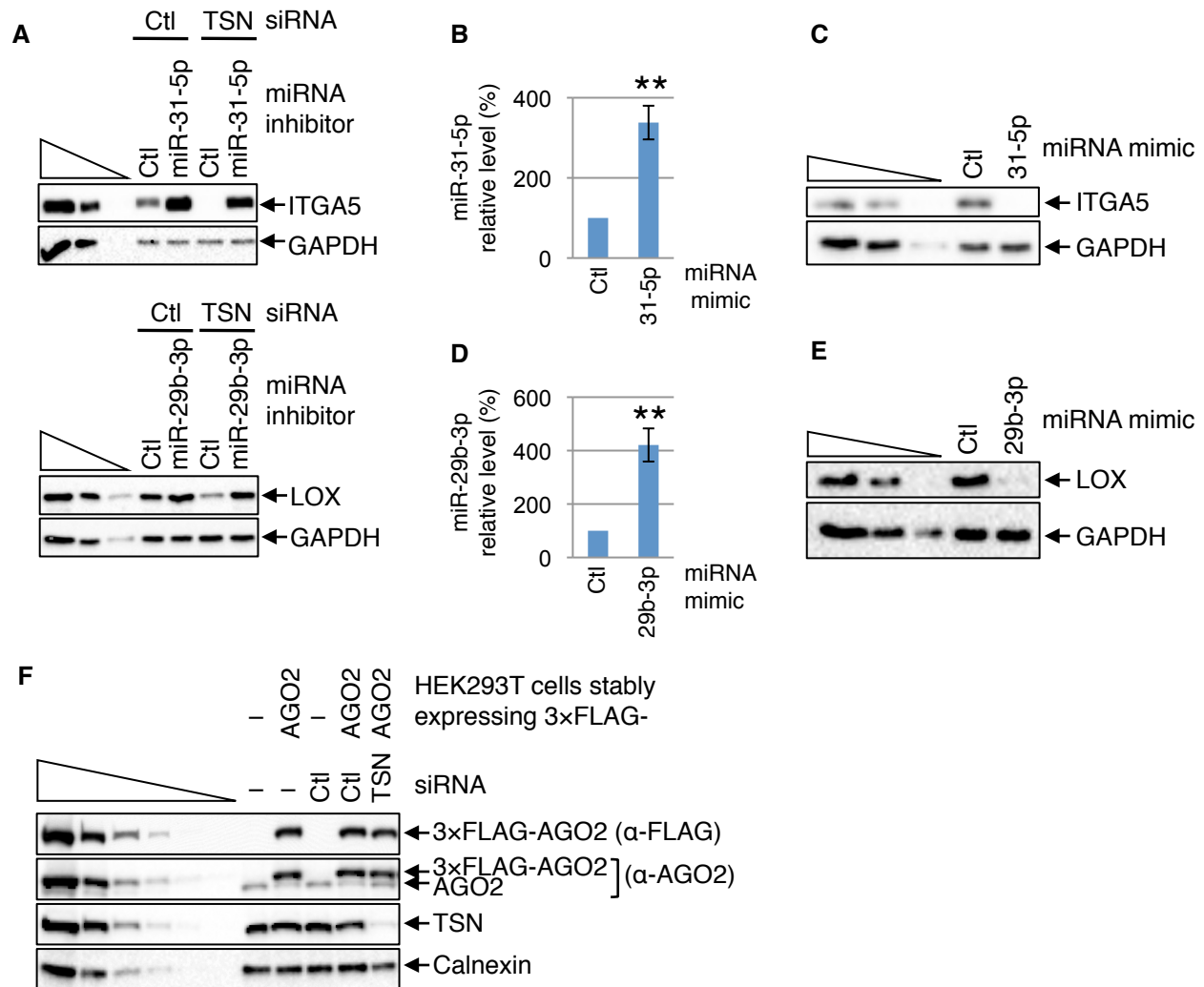
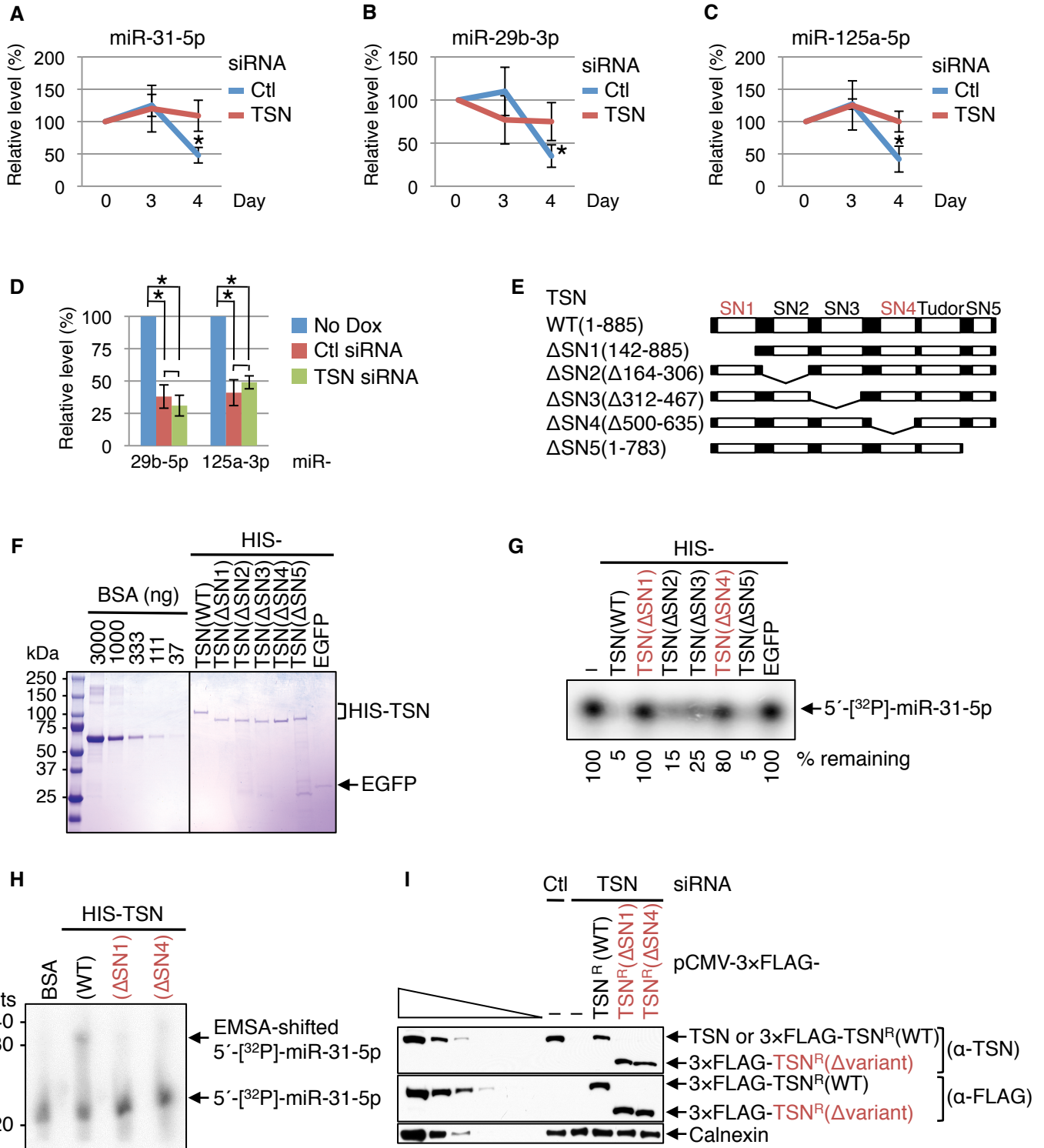


Fig. S3. Defining targets of miR-31-5p and miR-29b-3p in HEK293T cells

(A) WB demonstrating that the TSN siRNA-mediated decrease in the level of ITGA5 or LOX is reversed by co-transfecting cells with an inhibitor of miR-31-5p or miR-29b-3p, respectively. (B) Histogram representation of RT-qPCR results showing that exogenously introducing the miR-31-5p mimic into HEK293T cells increases the total-cell level of miR-31-5p ~3-fold relative to the level in Ctl siRNA-transfected cells. The miR-31-5p level is relative to the level of U6 snRNA, and the relative level in the presence of Ctl siRNA is defined as 100. (C) WB demonstrating that the miR-31-5p mimic inhibits the expression of cellular ITGA5 protein, which derives from an mRNA that is a target of miR-31-5p. (D) As in (B), but showing that exogenously introducing the miR-29b-3p mimic into HEK293T cells increases the total-cell level of miR-29b-3p ~4-fold relative to the level in Ctl siRNA-transfected cells. (E) WB demonstrating that the miR-29b-3p mimic inhibits the expression of cellular LOX protein, which derives from an mRNA that is a target of miR-29b-3p. (F) WB of HEK293T cells stably expressing 3×FLAG-AGO2 or, as a negative control, 3×FLAG. Cells were transiently transfected with Ctl siRNA or TSN siRNA. All results derive from ≥ 3 independent experiments. Histograms represent the average and SD. * $P < 0.05$, ** $P < 0.01$.



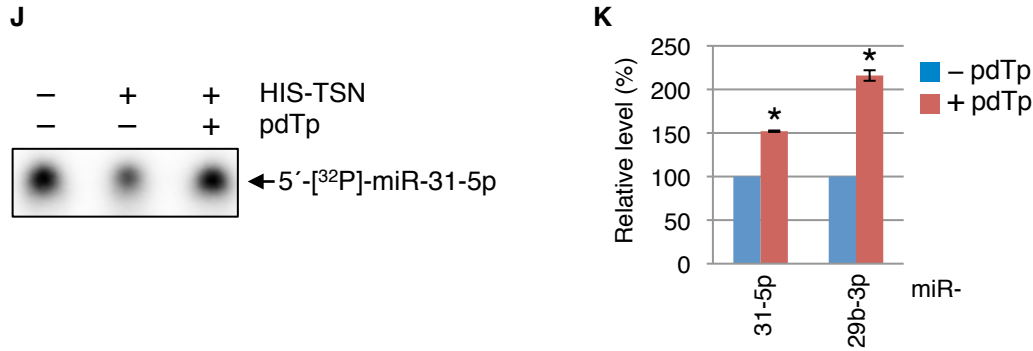


Fig. S4. TSN nuclease activity is required for cellular TumiD

(A-C) Plot of RT-qPCR results of the specified miRNAs after conditional knockdown of Dicer by Dox-induced expression of Dicer shRNA. Results show that miRNA decay, i.e. TumiD, is inhibited by TSN siRNA relative to Ctl siRNA. Cells were transfected with either TSN siRNA or Ctl siRNA and, 4-h later, medium was replaced with Dox-containing medium. Cells were harvested on the specified days. The level of each miRNA is relative to the level of U6 snRNA, and relative levels on day 0 (no Dox treatment) are defined as 100. (D) Histogram representation of RT-qPCR results showing that the miR-29b-5p (i.e. the miR* for miR-29b-3p) and miR-125a-3p (i.e. the miR* for miR-125a-5p) are not stabilized by TSN siRNA relative to Ctl siRNA in Dicer-depleted cells. miR-29b-5p and miR-125a-3p serve as internal controls for, respectively, miR-29b-3p and miR-125a-5p in experiments shown in Fig. 1E and fig. S4, B and C. Notably, miR-31-3p (i.e. the miR* for miR-31-5p) was not quantifiable. The level of each miRNA is relative to the level of U6 snRNA. Cells were harvested 4 days after Dox treatment. (E) Diagrams of wild-type (WT) TSN and the designated deletion variants, each of which lacks one of the staphylococcal-like nuclease (SN) domains. (F) Coomassie-blue staining of *E. coli*-produced HIS-TSN variants (2 pmol) and enhanced green fluorescent protein (EGFP). Lanes 2-6 analyzed 3-fold dilutions of bovine serum albumin (BSA). (G) HIS-TSN(Δ SN1) and HIS-TSN(Δ SN4), shown in red, are catalytically inactive variants of HIS-TSN. Assays were performed by incubating 5'-[³²P]-miR-31-5p with the designated *E. coli*-produced recombinant HIS-TSN variant or, as a negative control, *E. coli*-produced recombinant HIS-tagged EGFP. (H) Electrophoretic mobility shift assay (EMSA) showing that HIS-TSN(Δ SN1) and HIS-TSN(Δ SN4) fail to bind 5'-[³²P]-miR-31-5p miRNA, explaining at least in part why we observe them to be catalytically inactive. Calcium was omitted to inhibit TSN-mediated cleavage. (I) WB demonstrating that endogenous TSN was downregulated in TSN siRNA-treated cells and replaced with the designated TSN variant. Superscript R denotes resistance to TSN siRNA. (J) pdTp inhibits TSN-mediated degradation of 5'-[³²P]-labeled miR-31-5p *in vitro*. (K) Histogram representation of RT-qPCR results showing that the levels of miR-31-5p and miR-29b-3p increase in HEK293T cells that were treated with 200 μ M pdTp compared to untreated (-) cells. The level of each miRNA is relative to the level of U6 snRNA, and relative levels in untreated cells are defined as 100. All results derive from ≥ 3 independent experiments. Histograms represent the average and SD. * $P < 0.05$, ** $P < 0.01$.

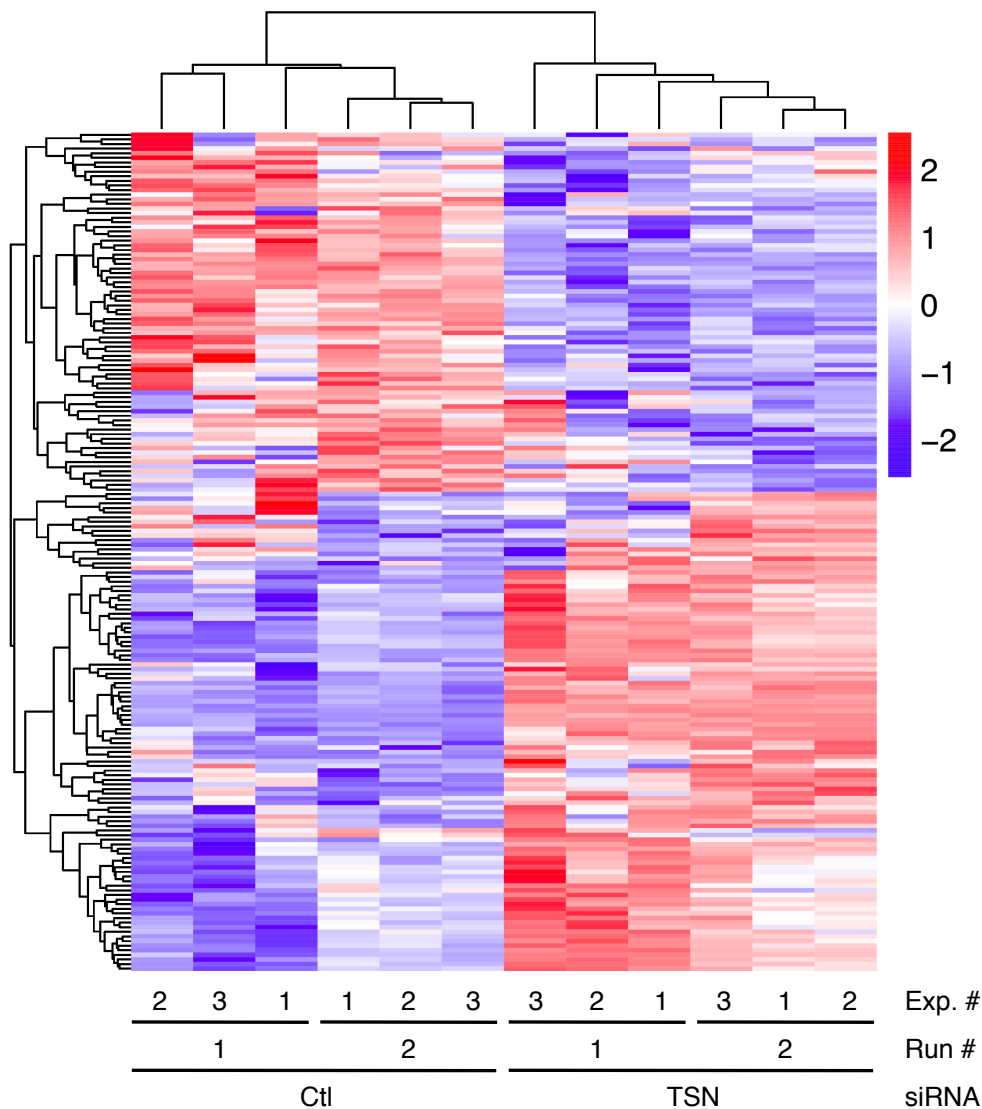


Fig. S5. Heat map of hierarchically clustered miRNA expression in the miR-seq data from Runs #1 and #2

Shown are 182 differentially expressed (adjusted P -value < 0.05) miRNAs in either miR-seq Run separately in the presence of TSN siRNA (Table S3). Color key represents row-scaled $r\text{Log}$ -transformed expression values after batch effect removal using Limma. We conclude that data sets from Run #1 and Run #2 show a high degree of consistency when these 182 differentially expressed miRNAs in TSN knockdown relative to Ctl knockdown samples are compared.

Notably, of those miRNAs that generated ≥ 10 raw reads, $\sim 28\%$ (44 miRNAs) and $\sim 27\%$ (80 miRNAs) were significantly upregulated in Run #1 and #2, respectively, and 32 miRNAs were in common to both Runs. The depth of coverage and mapping rates were higher in Run #2 relative to Run #1, which partially explains the larger number of putative TumiD targets identified in Run #2 (Fig. 2A and Tables S2 and S3).

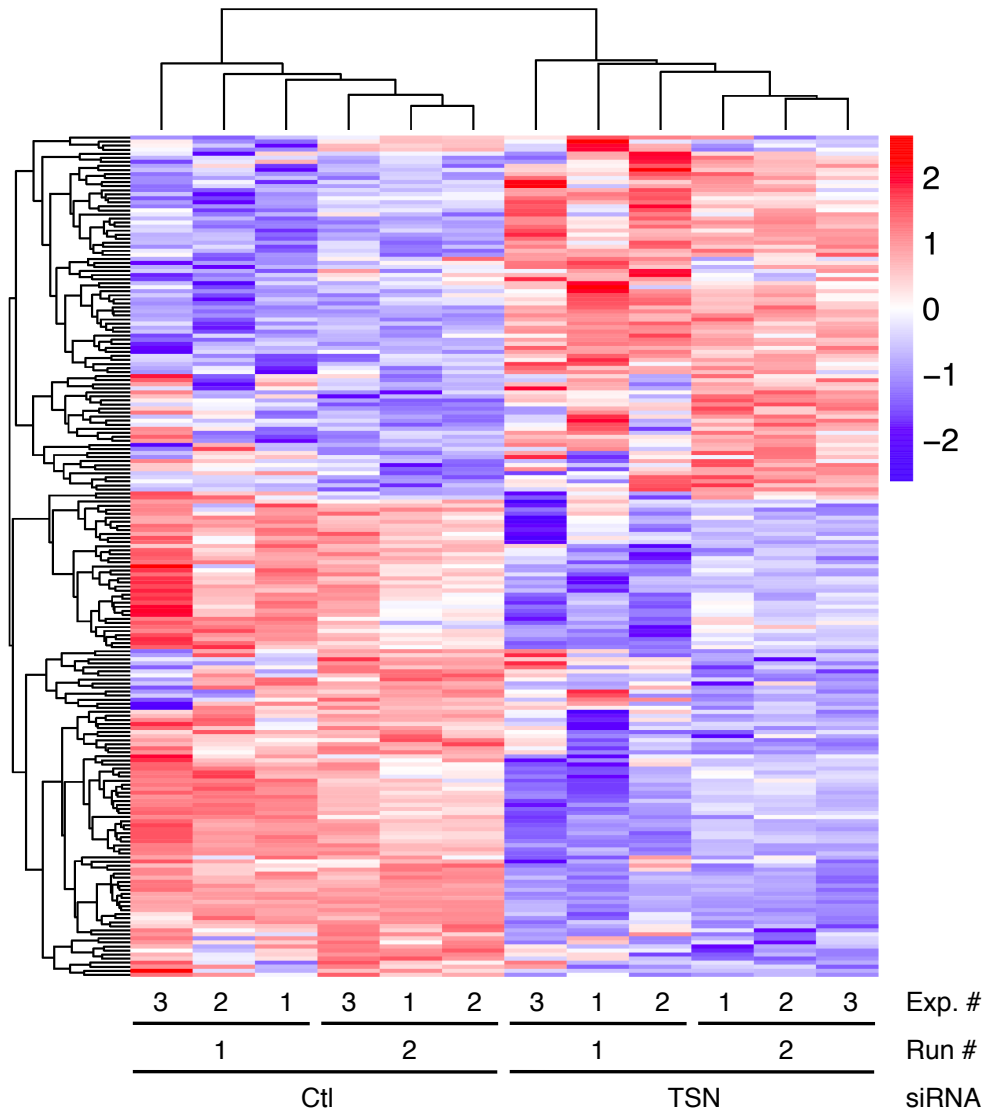


Fig. S6. Heat map of hierarchically clustered miRNA expression in the miR-seq data
 Shown are 208 differentially expressed (adjusted P -value < 0.05) miRNAs from either sequencing run separately or combined in the presence of TSN siRNA. Color key represents row-scaled rLog transformed expression values after batch correction.

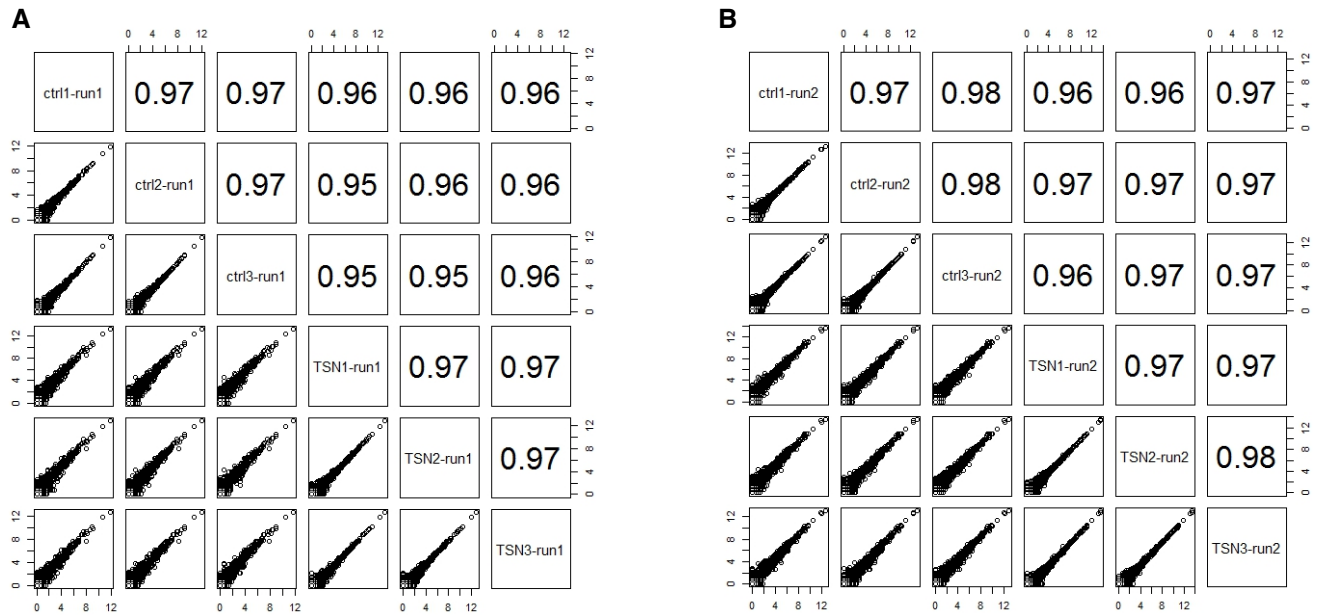
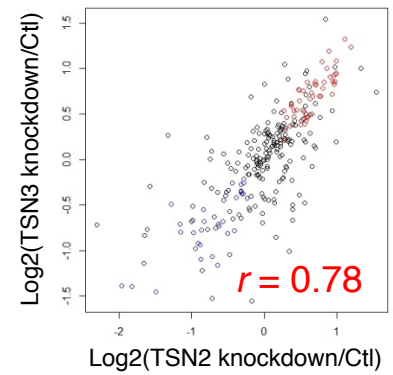
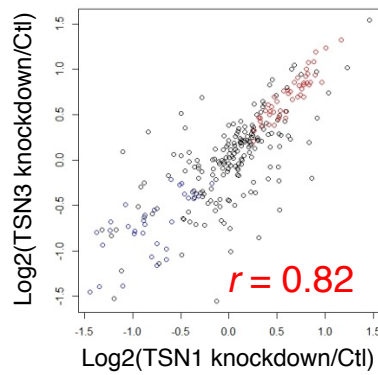
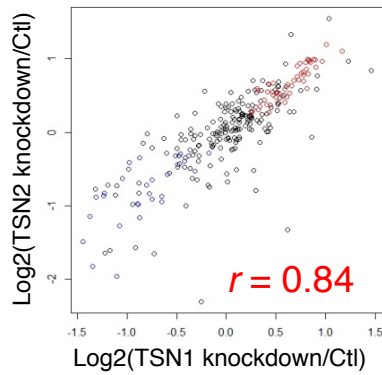


Fig. S7. Pairwise scatterplots of $\log_2(\text{raw count})$ for Run #1 (A) and Run #2 (B) for detected miRNAs (≥ 1 read)

Pearson correlation coefficient is > 0.95 among replicates within each Run.

A



B

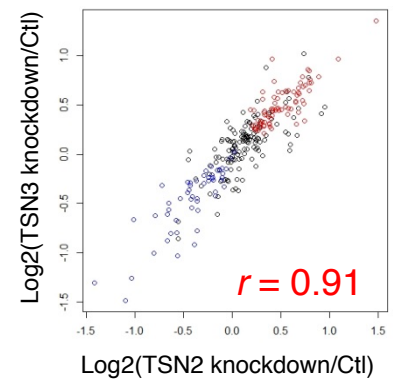
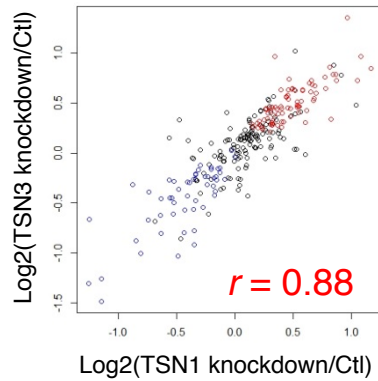
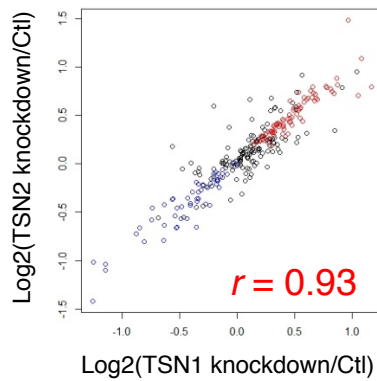


Fig. S8. Scatterplots of the changes (log₂ ratio) in miRNA abundance in the three replicates of TSN knockdown samples relative to Control (Ctl) knockdown samples in Run #1 (A) or Run #2 (B)

The Ctl value used is an average of three Ctl knockdown samples. miRNAs that were up- or down-regulated upon TSN knockdown ($P_{adj} < 0.05$) are in red or blue, respectively. The red “r” indicates that Pearson correlation coefficient.

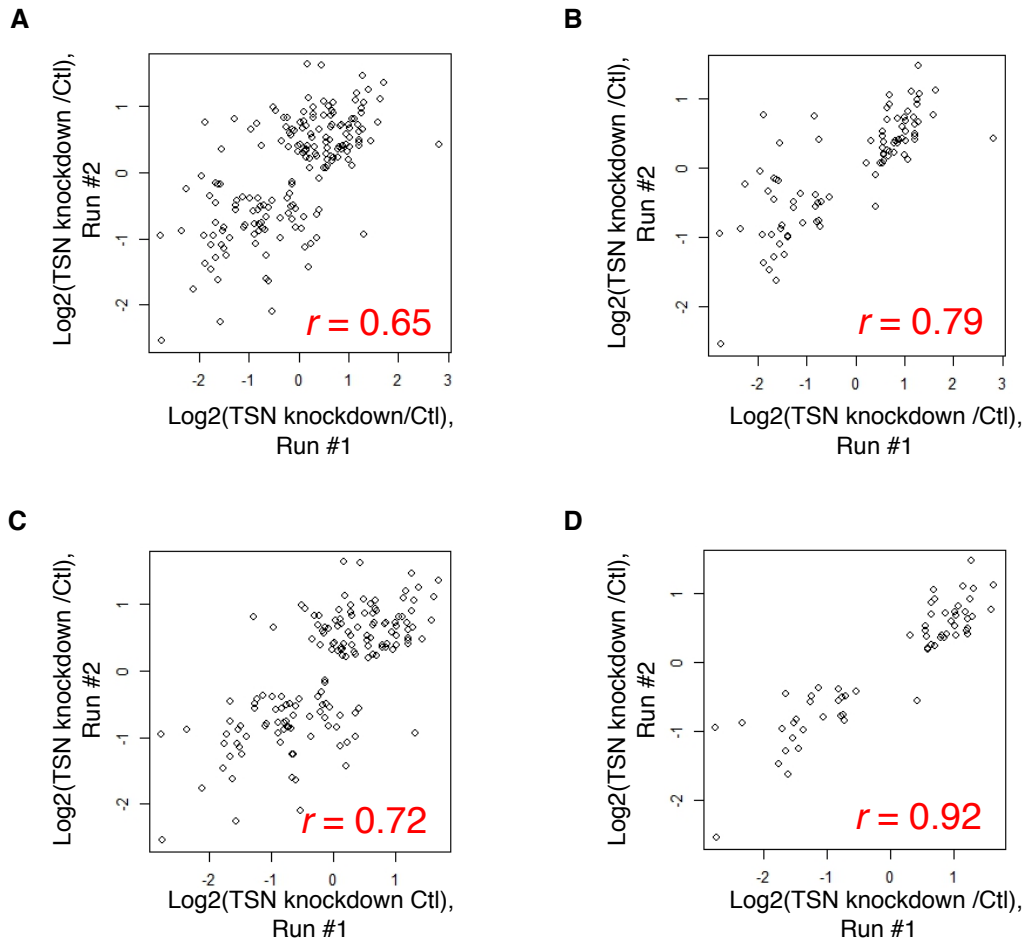


Fig. S9. Scatterplots comparing the changes (log₂ ratio) in miRNA abundance in the three replicates of TSN knockdown samples relative to Control (Ctl) knockdown samples between the two miR-seq Runs

(A) All detected miRNAs. (B) miRNAs with $P_{adj} < 0.05$ in Run #1. (C) miRNAs with $P_{adj} < 0.05$ in Run #2. (D) miRNAs with $P_{adj} < 0.05$ in both runs. In each case, the Ctl value used is an average of three Ctl knockdown samples in the specified Run. The red "r" indicates that Pearson correlation coefficient.

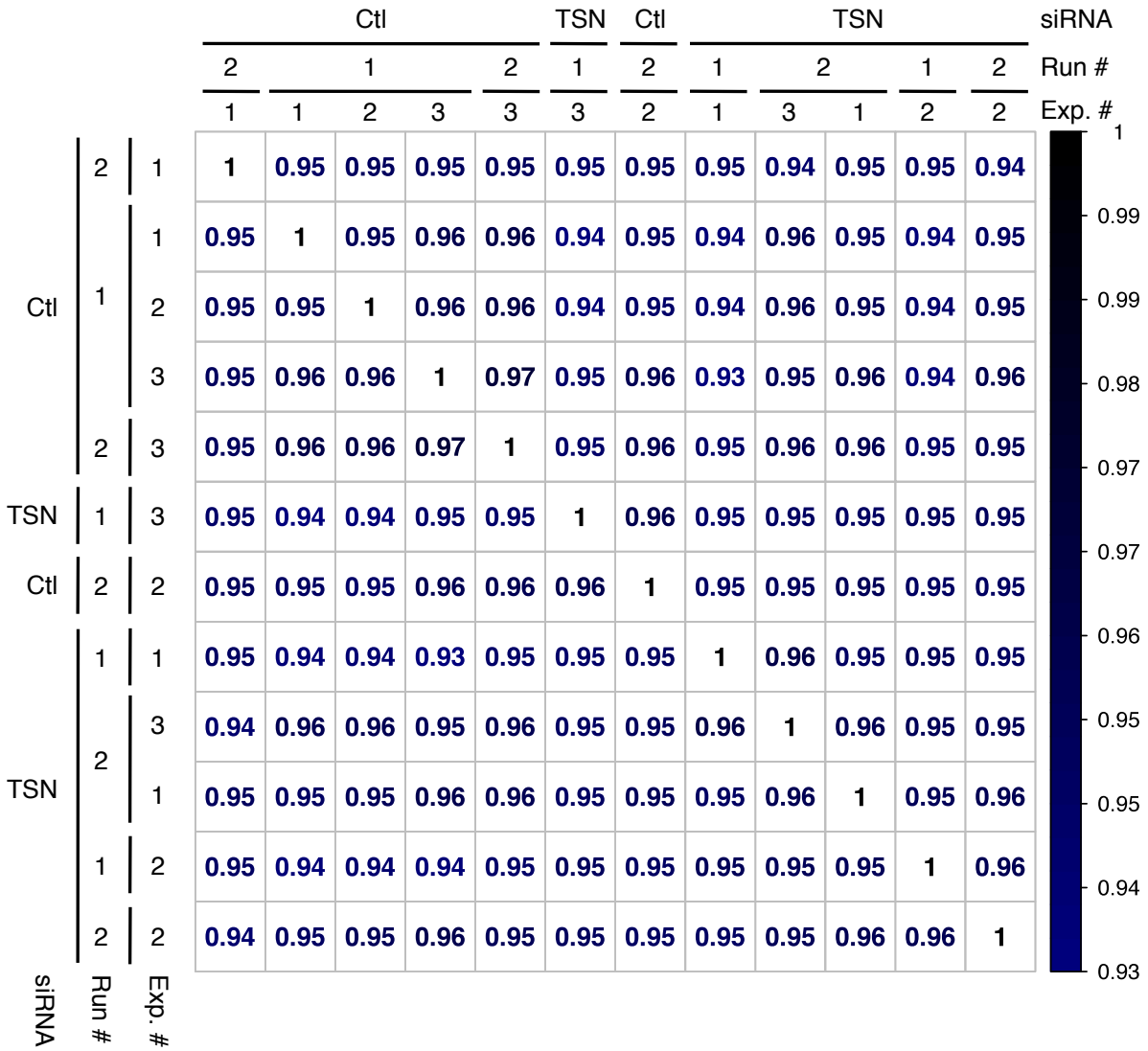


Fig. S10. Pair-wise Spearman correlation of miRNA levels in the miR-seq data after rLog transformation and batch correction, showing clustering of conditional groups

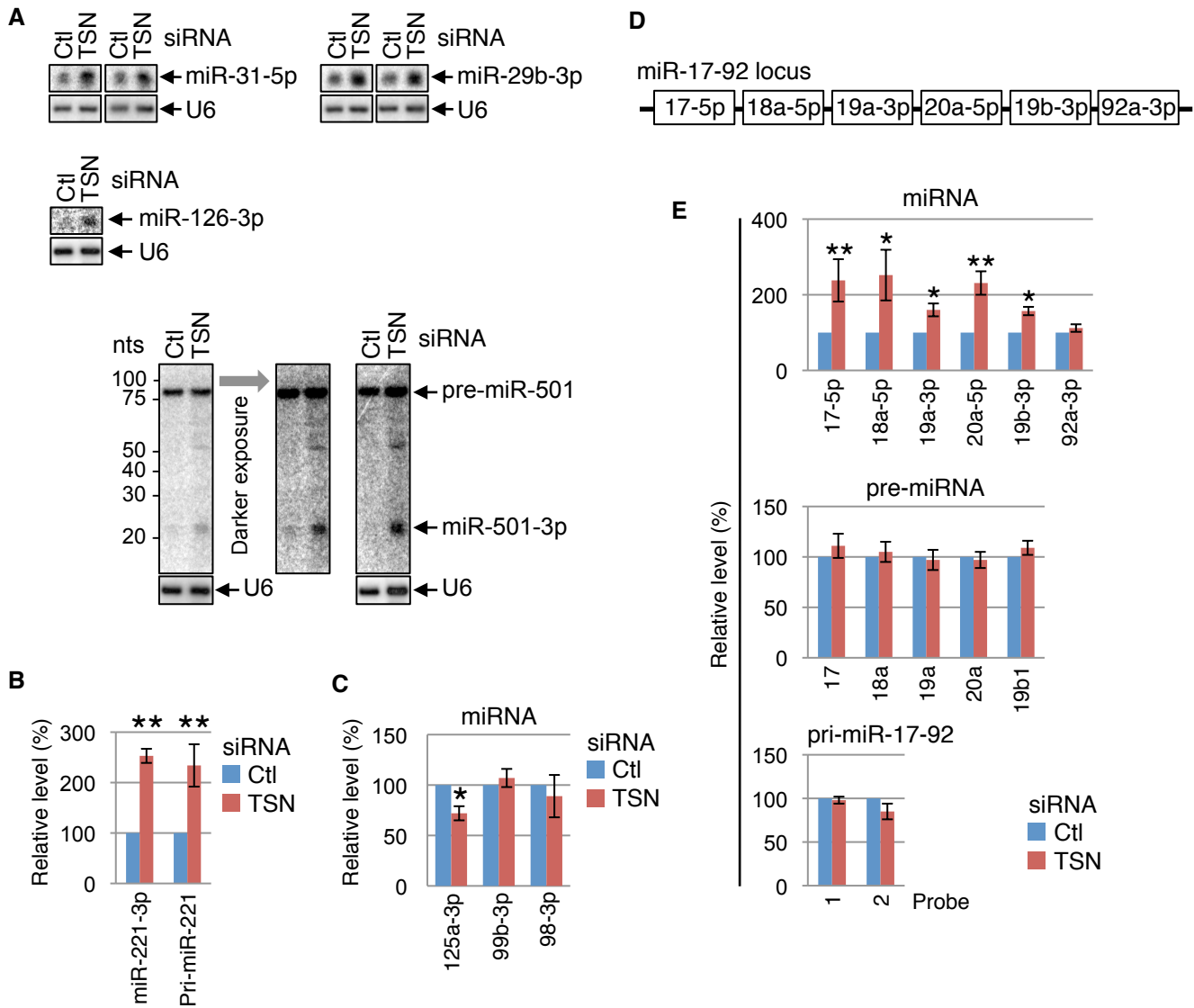


Fig. S11. Northern blotting and RT-qPCR corroboration of miR-seq data: identifying additional TumiD targets

(A) Northern blotting showing that the levels of mature miR-126-3p and miR-501-3p, both of which were identified as TumiD targets in miR-seq Runs #1 and #2 (Table S4), increase in TSN siRNA-transfected relative to Ctl siRNA-transfected HEK293T cells, while the levels of pre-miR-501 remain unchanged (pre-miR-126 was undetectable). Notably, while pre-miR-501 was easily detectable using Northern blotting, it was not quantifiable using RT-qPCR since the pre-designed primer pair generated non-specific RT-qPCR products. miR-31-5p and miR-29b-3p serve as positive TumiD controls (Fig. 1). (B) Histogram representation of RT-qPCR results showing that the levels of miR-221-3p and pri-miR-221 increase upon TSN knockdown. Notably, pre-miR-221 was undetectable. The level of miR-221-3p is relative to the level of U6 snRNA, the level of pri-miR-221 is relative to the level of β -actin mRNA, and relative levels in the presence of Ctl siRNA are defined as 100.

(C) Histogram representation of RT-qPCR results showing that the levels of miR-125a-3p (the miR* for miR-125a-5p), miR-99b-3p (the miR* for miR-99b-5p) and miR-98-3p (the miR* for miR-98-5p) do not increase upon TSN knockdown, indicating that TumiD degrades mature miRNAs. The level of each miRNA is relative to the level of U6, and relative levels in the presence of Ctl siRNA are defined as 100. (D) Diagram of the miR-17-92 cluster. (E) Histogram representations of RT-qPCR results demonstrating that the levels of individual miRNAs in the miR-17-92 cluster respond differently to TSN knockdown while the level of their individual pre-miRNAs and the common cluster pri-miRNA remained unchanged upon TSN knockdown. Two different Taqman probes were used to measure the level of the cluster pri-miRNA.

All results derive from ≥ 3 independent experiments. Histograms represent the average and SD.

* $P < 0.05$, ** $P < 0.01$.

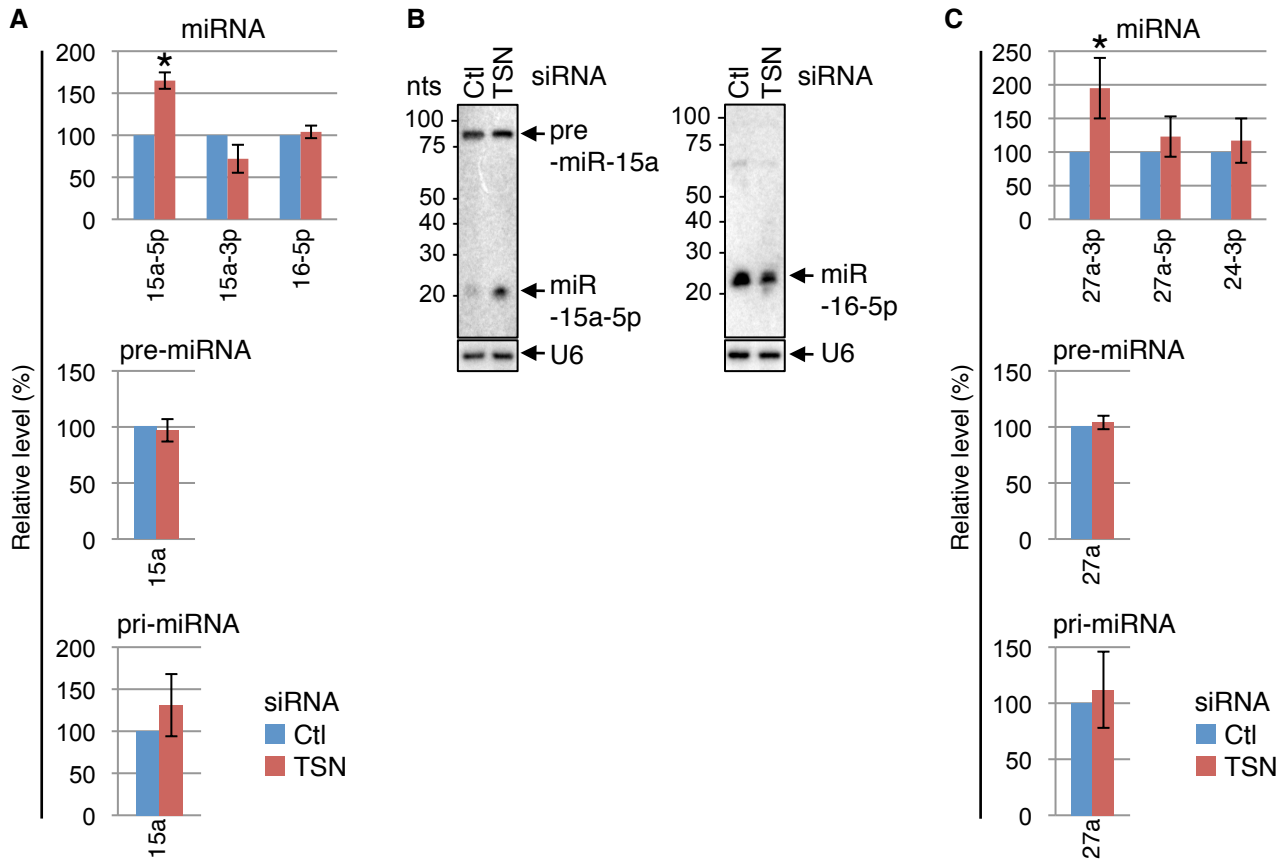


Fig. S12. Northern blotting and RT-qPCR corroboration of miR-seq data: Confirming new TumiD targets identified in Run #2

(A) Histogram representations of RT-qPCR results demonstrating that the level of mature miR-15a-5p, which was defined as a TumiD target in miR-seq Run #2 (Table S3), increases upon TSN knockdown, while the levels of its miR* (miR-15a-3p), pre-miRNA, and pri-miRNA do not significantly change; the level of miR-16-5p, which is encoded in the same miRNA cluster as miR-15a-5p, likewise does not change. miRNAs and pre-miRNAs levels are relative to the level of U6 snRNA, pri-miRNA levels are relative to the level of β -actin mRNA, and relative levels in the presence of Ctl siRNA are defined as 100. (B) Northern blotting corroborating that the level of the TumiD target miR-15a-5p increases upon TSN knockdown, while the levels of pre-miR-15a and miR-16-5p do not increase. (C) Histogram representations of RT-qPCR results demonstrating that the level of mature miR-27a-3p, which was defined as TumiD target in miR-seq Run #2 (Table S3), increases upon TSN knockdown, while the levels of its miR* (miR-27a-5p), pre-miRNA and pri-miRNA do not significantly change; the level of miR-24-3p, which is encoded in the same miRNA cluster as miR-27a-3p, likewise does not change. miRNA and pre-miRNA levels are relative to the level of U6 snRNA, pri-miRNA levels are relative to the level of β -actin mRNA, and relative levels in the presence of Ctl siRNA are defined as 100. All results derive from ≥ 3 independent experiments. Histograms represent the average and SD. * $P < 0.05$, ** $P < 0.01$.

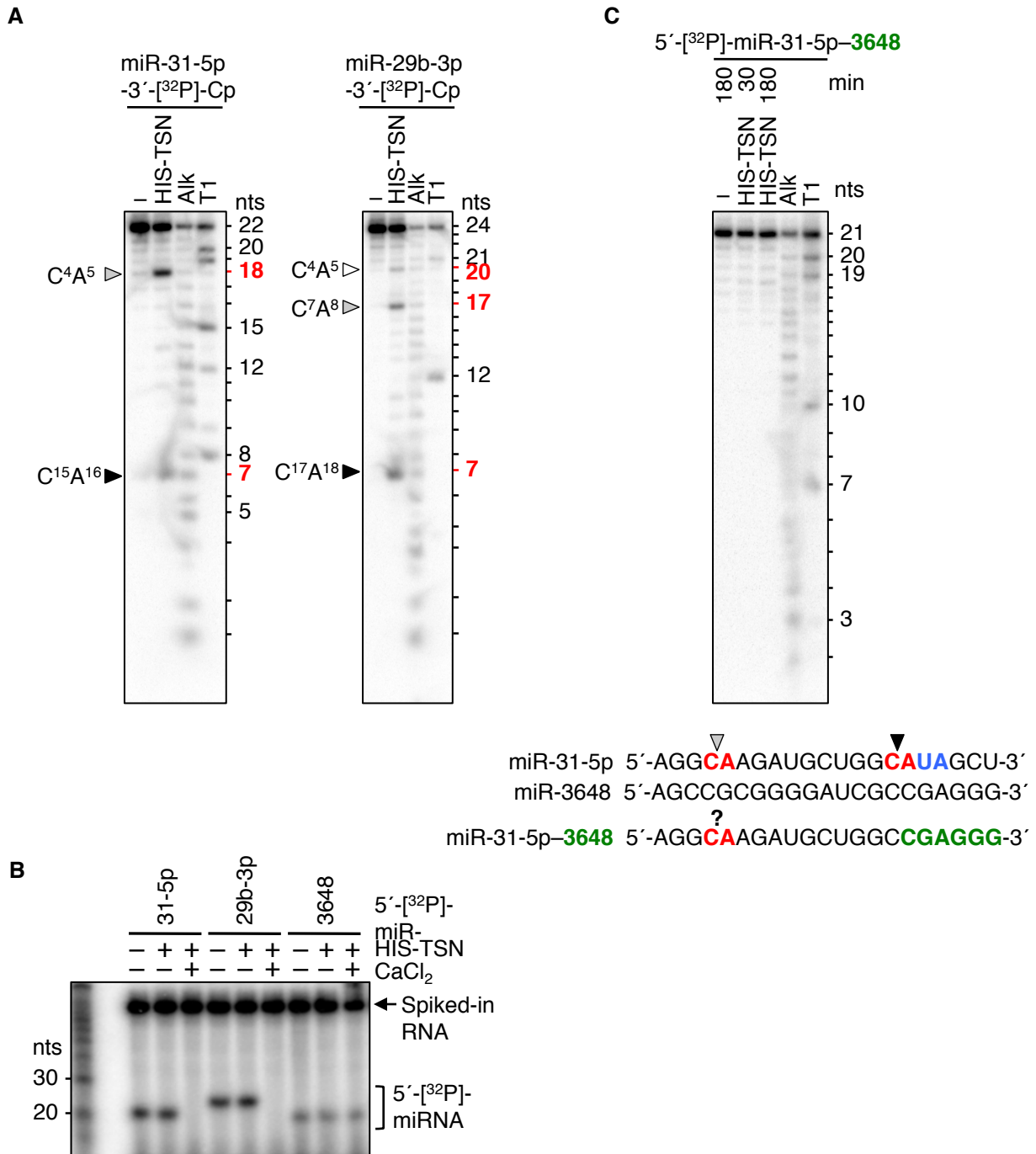
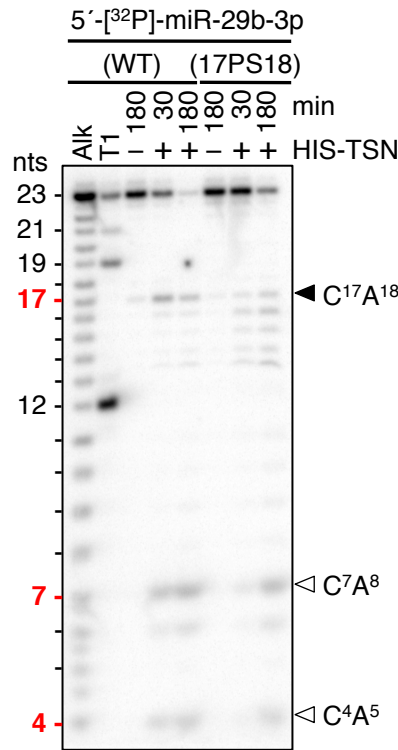


Fig. S13. TSN endonucleolytic activity cleaves miRNAs at CA phosphodiester bonds

(A) *E. coli*-produced HIS-TSN was incubated with 3'-[³²P]Cp-labeled miR-31-5p (left panel) or 3'-[³²P]Cp-labeled miR-29b-3p (right panel) for 30 min, and reaction products were subsequently phosphorimaged after separation in sequencing gels. Importantly, 3'-[³²P]Cp-labeling increases the length of each miRNA and, thus, the size of the observed cleavage products by one nucleotide. The rightmost two lanes of each gel represent, respectively, RNase T1 digestion (T1)

or alkaline hydrolysis (Alk) of the 3'-[³²P]Cp-labeled miRNA. Black, grey and white arrowheads denote strong, medium-strength and weak cleavage sites, respectively, and superscript numbers denote nucleotide position within each miRNA. Positions of CA dinucleotides are shown in red. Note that cleavage at C⁴A⁵ in miR-31-5p may be an exception to our finding that the 5'-most five nucleotides of a miRNA are inefficiently cleaved. **(B)** TSN-mediated degradation requires Ca⁺², and miR-3648 that lacks CA or UA is resistant to TSN-mediated degradation. The designated 5'-[³²P]-labeled miRNAs were incubated for 2 h with HIS-TSN in the absence (-) or presence (+) of CaCl₂ (5 mM). Reactions were terminated and spiked with an internally [³²P]-labeled RNA prior to RNA extraction. **(C)** Swapping the six 3'-most nucleotides in miR-31-5p, which include one susceptible CA bond, with the corresponding region of miR-3648 (green), which lacks a CA or UA dinucleotide, inhibits TSN-mediated cleavage in the swapped region (compare to HIS-TSN-mediated cleavage of miR-31-5p at C¹⁵A¹⁶ in Fig. 3A). The hybrid miRNA 5'-[³²P]-miR-31-5p-3648 was incubated with HIS-TSN for the specified time (min), and analyzed as in (A). Note that here and elsewhere, the relative intensities of cleavage products ≤ 5 nucleotides are not always reliable, explaining “?” over CA shown in red. All results are representative of ≥ 3 independent experiments.



miR-29b-3p(WT) 5'-UAG**CACCA**UUUGAAAUCAGUGUU-3'
 miR-29b-3p(17PS18) 5'-UAG**CACCA**UUUGAAAUCCAGUGUU-3'

Fig. S14. TSN endonucleolytic activity cleaves a phosphodiester bond more efficiently than a phosphorothioate bond

The designated variants of 5'-[³²P]-labeled miR-29b-3p were incubated with HIS-TSN for the specified times, and reaction products were separated in a sequencing gel and phosphorimaged. (17PS18) indicates that the phosphodiester bond between miR-29b-3p nucleotides 17 and 18 was replaced with a phosphorothioate bond (underlined in the sequence below the gel). The leftmost two lanes represent, respectively, alkaline hydrolysis (Alk) or RNase T1 digestion (T1) of 5'-[³²P]-miR-29b-3p. Black and white arrowheads mark strong and weak cleavage sites, respectively, and superscript numbers denote nucleotide position within each miRNA. CA dinucleotides and their positions are shown in red. Results are representative of 3 independently performed experiments.

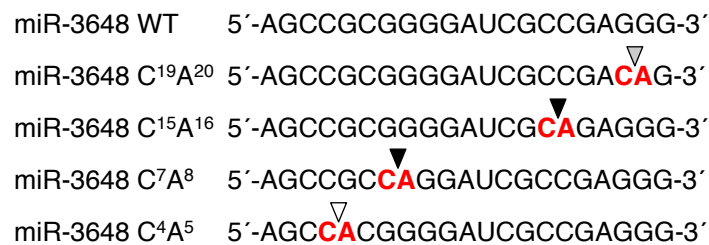
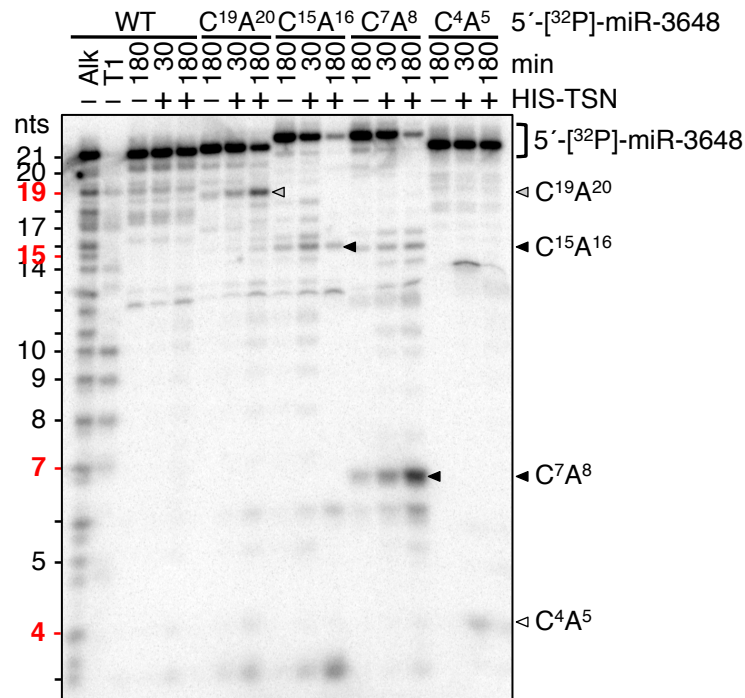


Fig. S15. Introducing a CA dinucleotide into a TumiD-resistant miRNA induces TSN-mediated cleavage at the introduced CA bond *in vitro*

Essentially as in fig. S14 but using WT or the designated variants of 5'-[³²P]-miR-3648, where the specified dinucleotide has been converted to CA. Black, grey and white arrowheads denote strong, medium-strength and weak cleavage sites, respectively. CA dinucleotides and their positions are shown in red. Results are representative of 3 independently performed experiments.

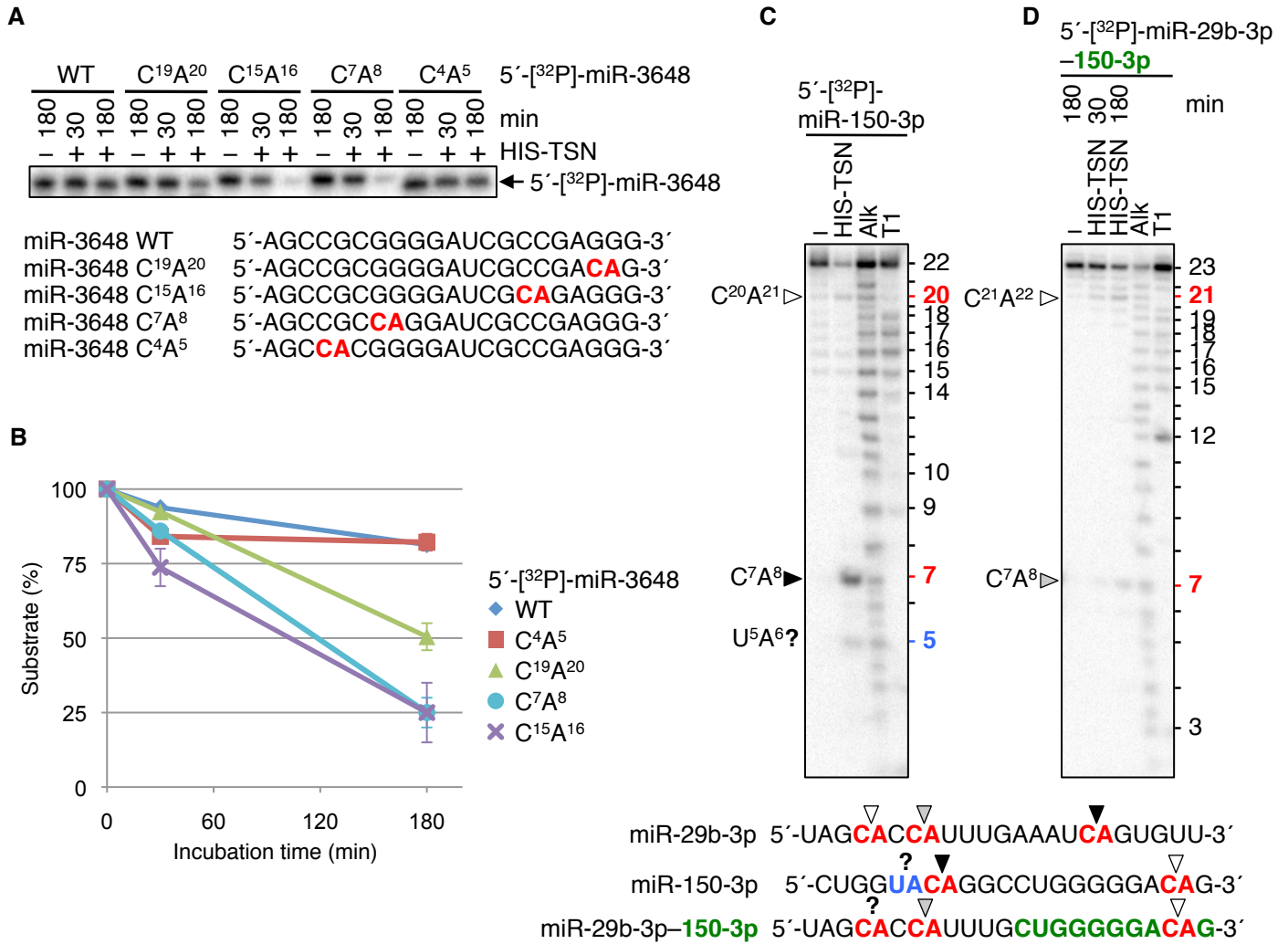


Fig. S16. A CA dinucleotide within the 5'-most or the 3'-most five nucleotides of a miRNA is least susceptible to HIS-TSN cleavage

(A) Essentially as in fig. S15 but measurements were confined to the loss of full-length 5'-[³²P]-miR-3648 variants. (B) Quantitations of results shown in A, where the amount of each 5'-[³²P]-miR-3648 at 0 min is defined as 100. (C) Essentially as in fig. S15 but 5'-[³²P]-miR-150-3p was used. Results show that miR-150-3p is cleaved efficiently at C⁷A⁸ but only weakly at C²¹A²², which is located within the 3'-most five nucleotides. (D) As in (C) but 5'-[³²P]-miR-29b-3p-150-3p hybrid miRNA was used. Results show that swapping the eleven 3'-most nucleotides of the 23-nucleotide miR-29b-3p, which contains C¹⁷A¹⁸, with the corresponding region of miR-150-3p (green), which contains CA within the 3'-most five nucleotides, abolished cleavage in the swapped region (compare to HIS-TSN-mediated cleavage of miR-29b-3p at C¹⁷A¹⁸ in Fig. 3A). CA and UA dinucleotides and their positions are shown in red and blue, respectively. Black, grey and white arrowheads denote strong, medium-strength and weak cleavage sites, respectively. Results derive from 3 independently performed experiments.

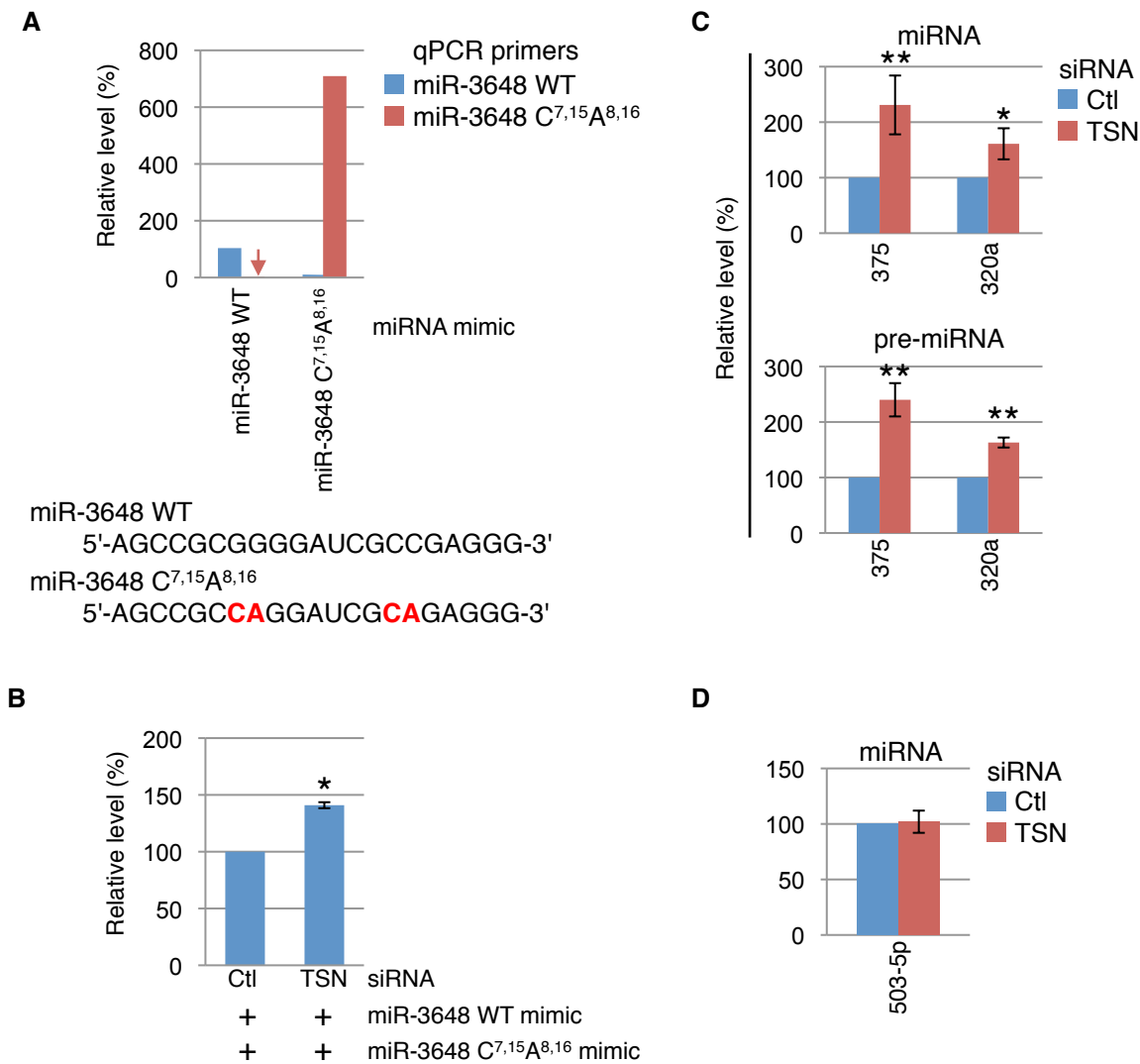


Fig. S17. Inserting CA dinucleotides into a TumiD-resistant miRNA can convert it to a TumiD target in cells; and TSN siRNA-mediated changes in the levels of the specified CA- and UA-lacking mature miRNAs are not due to TumiD

(A) Histogram representation of RT-qPCR results showing the specificity of the qPCR primers used to quantitate exogenously introduced miR-3648 WT and its CA-insertion variant miR-3648 C^{7,15}A^{8,16}. Primer specificity was evidenced by the fact that each primer pair detected only the corresponding miRNA mimic, introduced at 10 nM. The level of each miRNA is relative to the level of U6 snRNA, and relative levels in untransfected cells are defined as 1. Notably, the signal obtained for miR-3648 C^{7,15}A^{8,16} in cells transfected with miR-3648 WT mimic (red arrow) was not above background. (B) Histogram representation of RT-qPCR results showing that the level of miR-3648 C^{7,15}A^{8,16} was significantly increased in TSN siRNA-transfected HEK293T cells relative to Ctl siRNA-transfected cells. The level of miR-3648 C^{7,15}A^{8,16} is relative to the level of

the co-transfected TumiD-resistant miR-3648 WT, each introduced at 0.2 nM, and the relative level in the presence of Ctl siRNA is defined as 100. (C) Histogram representation of RT-qPCR results showing that increased levels of miR-375 and miR-320a upon TSN knockdown are due to changes in the levels of their pre-miRNAs. The level of each miRNA and pre-miRNA is relative to the level of U6 snRNA, and relative levels in the presence of Ctl siRNA are defined as 100. (D) Histogram representation of RT-qPCR results showing that the level of miR-503-5p remains unchanged upon TSN knockdown. The level of miR-503-5p is relative to the level of U6 snRNA, and relative level in the presence of Ctl siRNA is defined as 100.

All results derive from ≥ 3 independent experiments. Histograms represent the average and SD.

* $P < 0.05$, ** $P < 0.01$.

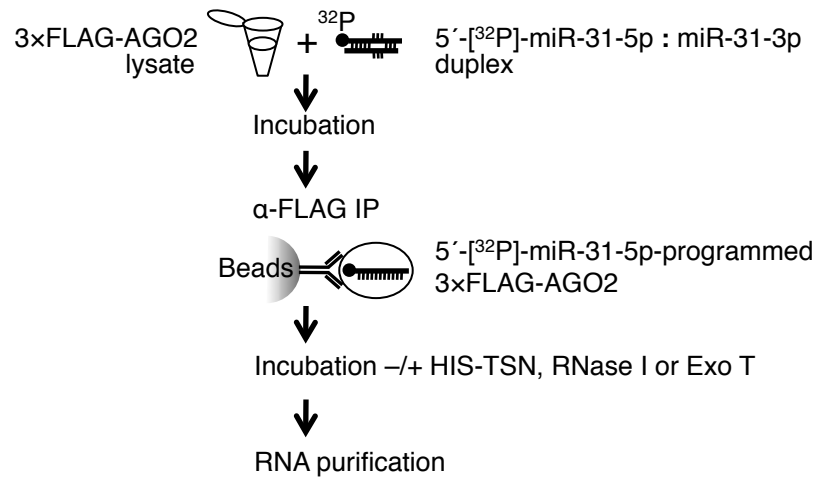


Fig. S18. Flow chart for experiment in Fig. 3E, which analyzes the susceptibility of AGO2-loaded miRNAs to cleavage by various nucleases *in vitro*

Lysates of HEK293T cells stably expressing 3xFLAG-AGO2 were incubated, i.e. “programmed”, with 5'-[^{32}P]-labeled miR-31-5p : miR-31-3p duplexes, and 3xFLAG-AGO2 was immunoprecipitated using α -FLAG. 3xFLAG-AGO2 IPs were incubated with recombinant HIS-TSN, RNase I or Exo T, and RNA was subsequently purified.

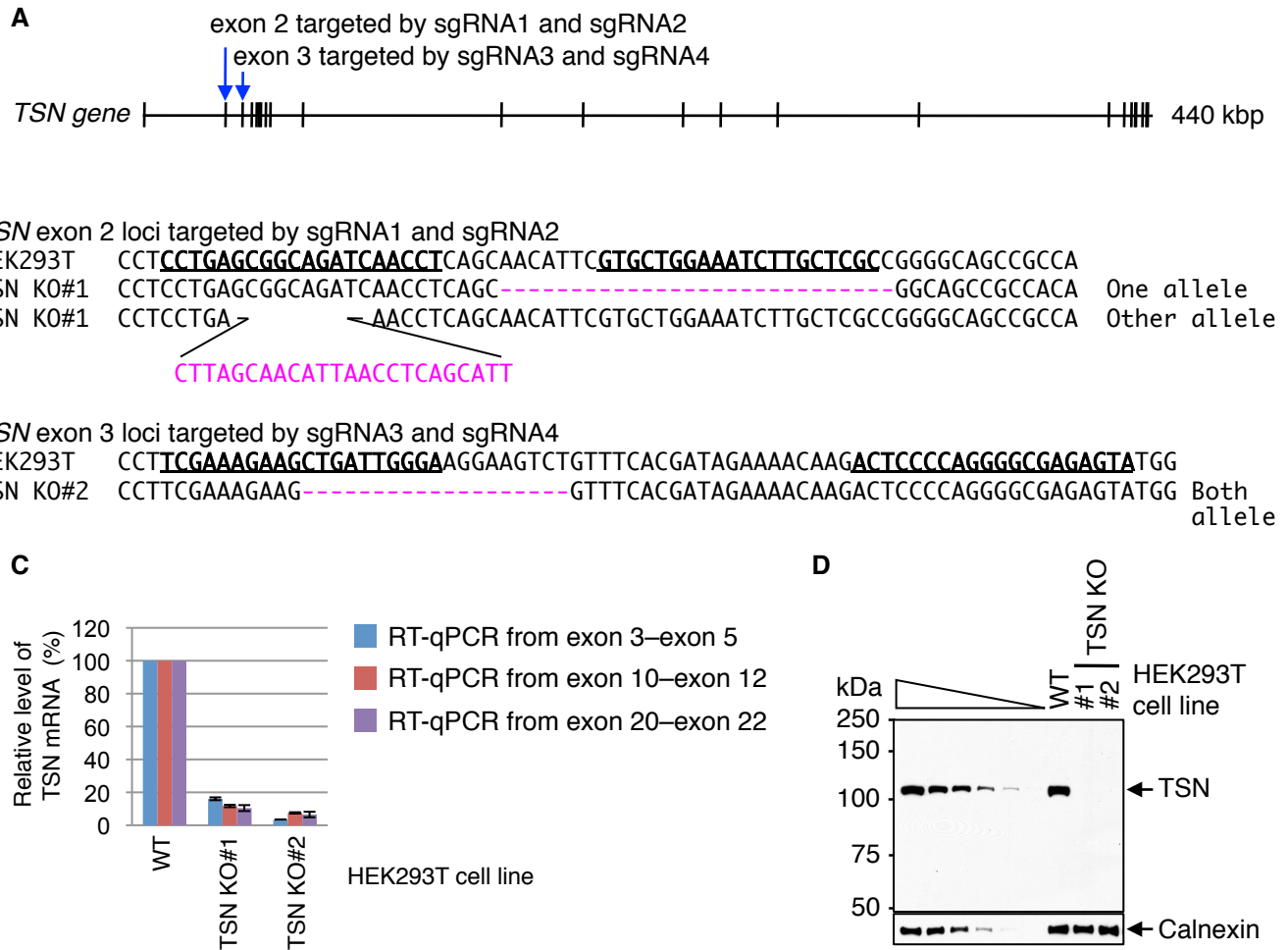


Fig. S19. Generation and analysis of TSN KO HEK293T cells

(A) Schematic diagram of the *TSN* gene and the loci targeted by each sgRNA pair. sgRNA1 and sgRNA2 were used to generate the TSN KO#1 cell line, while sgRNA3 and sgRNA4 were used to generate the TSN KO#2 cell line. (B) *TSN* gene sequencing results using WT, TSN KO#1 and TSN KO#2 cells. Sequences in the protein-coding region of the *TSN* gene targeted by each pair of sgRNAs are underlined. For TSN KO#1 cells, pink dashes denote deleted sequences in one *TSN* allele, and pink nucleotides specify the insertion in the other *TSN* allele. For TSN KO#2 cells, both *TSN* alleles harbor the same deletion, denoted by pink dashes. (C) Histogram representation of RT-qPCR results showing that the level of *TSN* mRNA is downregulated in TSN KO#1 and #2 cell lines relative to WT cells. RT-qPCR analyses spanned exon 3 to exon 5, exon 10 to exon 12, or exon 20 to exon 22 (Table S8). The level of *TSN* mRNA is relative to the level of GAPDH mRNA, and the relative level in WT cells is defined as 100. (D) WB demonstrating CRISPR-Cas9-mediated *TSN* knockout (KO) in independently generated cell lines (#1 and #2), each using different sgRNAs pairs. All results derive from ≥ 3 independent experiments. Histograms represent the average and SD.

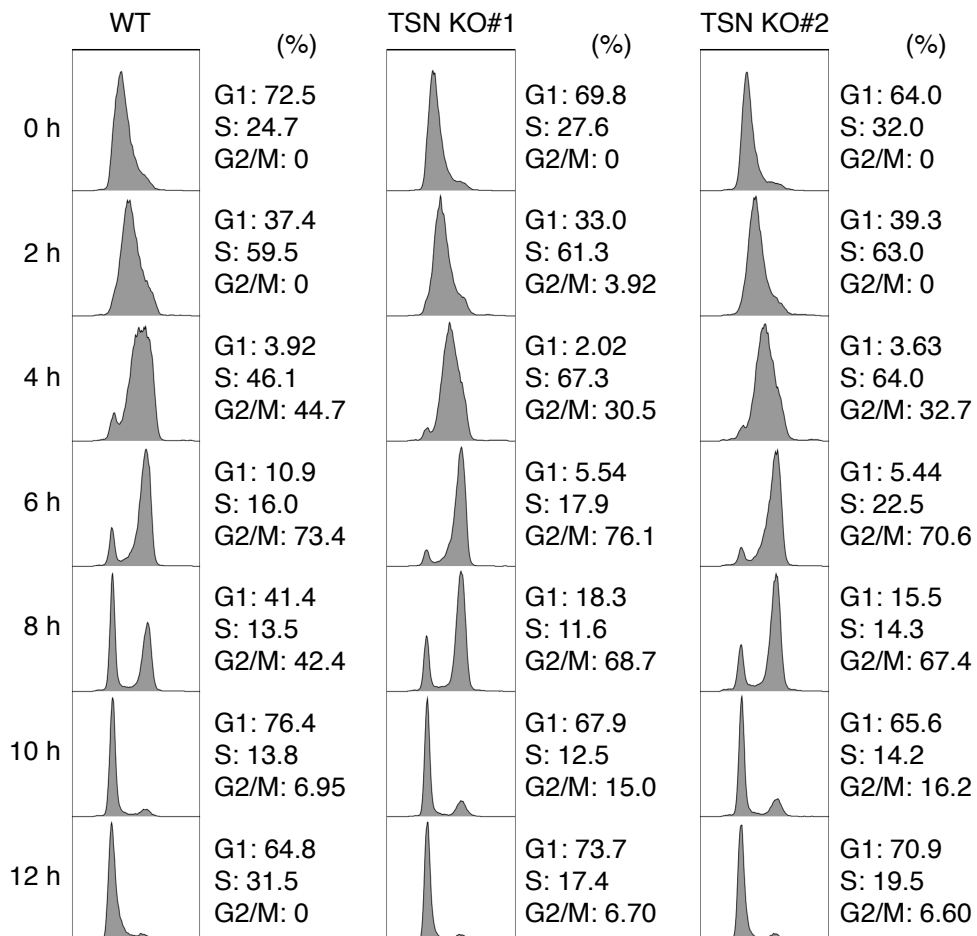


Fig. S20. The cell cycle is prolonged in TSN KO HEK293T cells relative to WT HEK293T cells

Flow cytometry analyses where TSN KO#1, TSN KO#2 and WT cells were synchronized in G1/S using a double-thymidine block, released from synchronization, and analyzed at the designated time. Results are representative of 3 independently performed experiments.

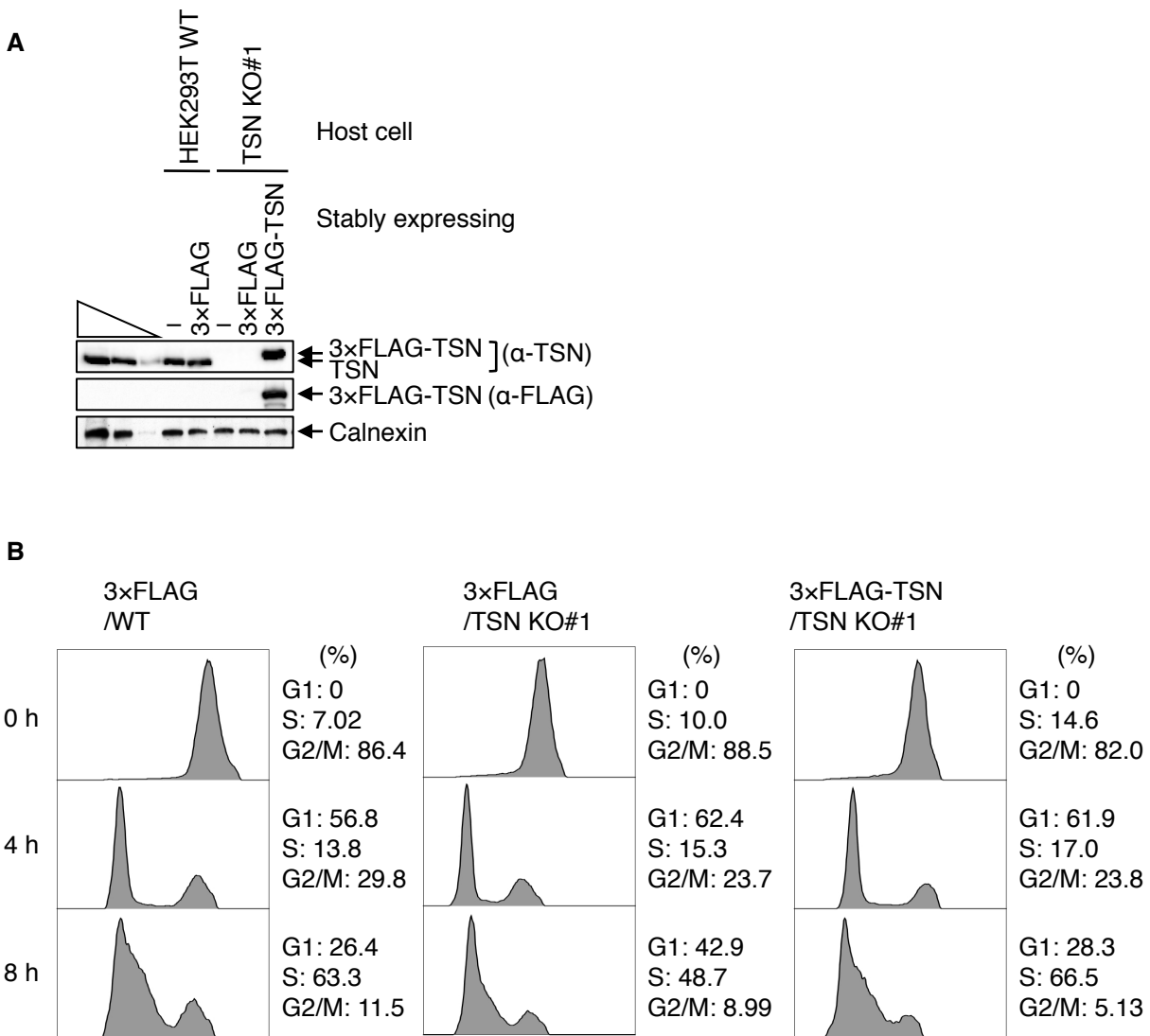


Fig. S21. Stably expressing FLAG-TSN in TSN KO HEK293T cells restores the rate of G1/S progression to normal

(A) WB demonstrating stable expression of 3×FLAG-TSN in TSN KO#1 cells. WT and TSN KO#1 cells that stably express 3×FLAG were used as control. (B) Flow cytometry analyses where WT cells expressing 3×FLAG, TSN KO#1 cells expressing 3×FLAG, or TSN KO#1 cells expressing 3×FLAG-TSN were synchronized in G2/M using nocodazole, released from synchronization, and analyzed at the designated times. The percent (%) of cells in each cell-cycle phase is shown. Results are representative of 3 analyzed clones.

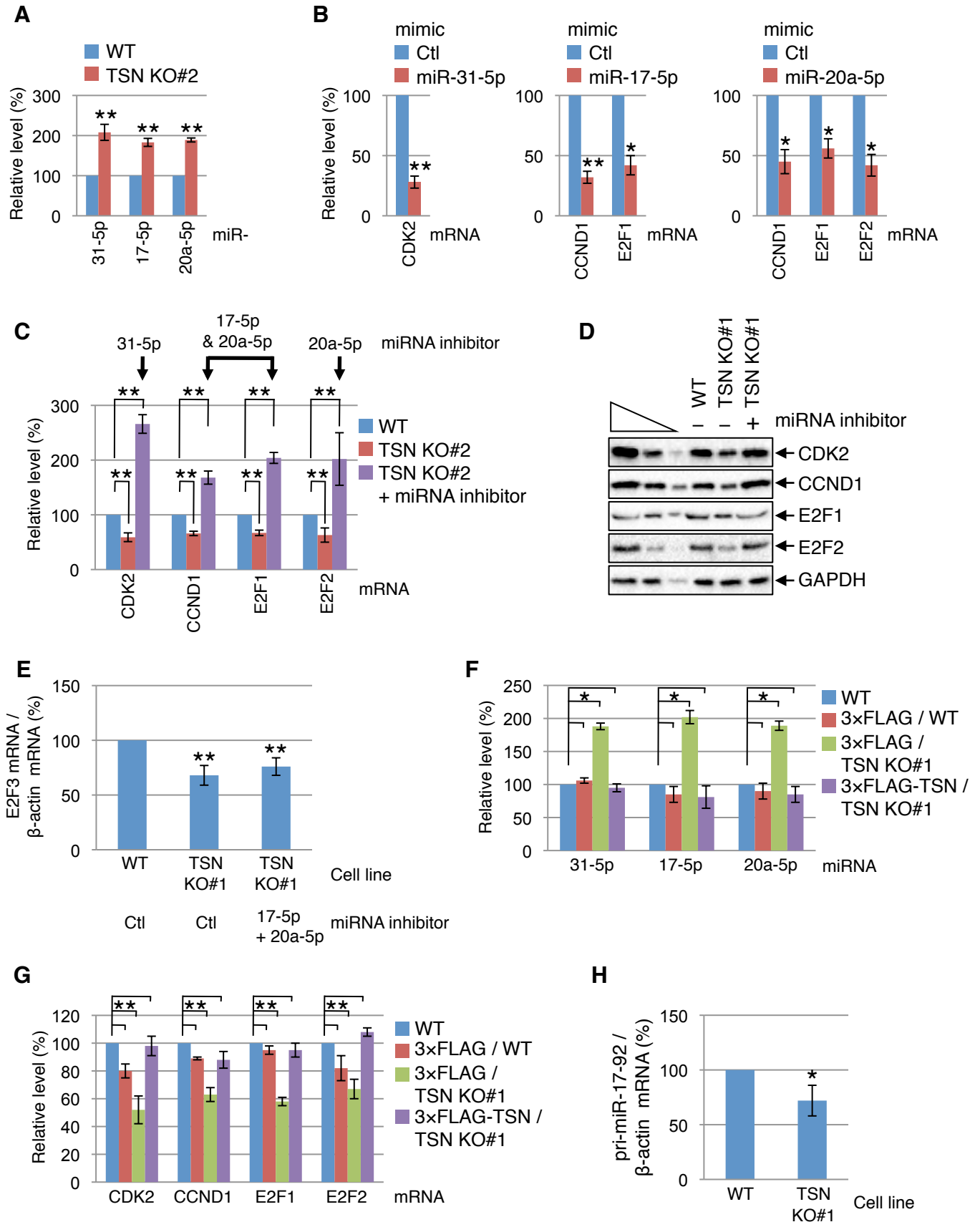


Fig. S22. TumiD targets are upregulated and mRNAs encoding proteins critical to G1-to-S phase progression are, as a consequence, downregulated in TSN KO cells

(A) Histogram representation of RT-qPCR results showing upregulation of the specified TumiD targets in TSN KO#2 cells compared to WT cells. Cells were synchronized in G1/S using a double-thymidine block. The level of each miRNA is relative to the level of U6 snRNA, and relative levels in WT cells are defined as 100. (B) Histogram representation of RT-qPCR results showing that a miR-31-5p mimic, miR-17-5p mimic, and miR-20a-5p mimic, relative to a Ctl mimic, downregulate their target mRNAs. (C) Histogram representation of RT-qPCR results demonstrating that the levels of CDK2, CCND1, E2F1 and E2F2 mRNAs are downregulated in TSN KO#2 cells compared to WT cells that were synchronized in G1/S using a double-thymidine block, and that transfecting TSN KO#2 cells with the corresponding miRNA inhibitors rescues the levels of CDK2, CCND1, E2F1 and E2F2 mRNAs. The level of each mRNA is relative to the level of β -actin mRNA, and relative levels in WT cells are defined as 100. (D) WB confirming coordinate effects on the proteins encoded by mRNAs analyzed in (C). (E) Essentially as in (C) but showing that the reduced expression of E2F3 mRNA in KO#1 cells compared to WT cells is not rescued upon transfecting TSN KO#1 cells with miR-17-5p and miR-20a-5p inhibitors. (F) Essentially as in (A) but showing that expressing 3 \times FLAG-TSN in TSN KO#1 cells rescues the levels of the specified TumiD targets compared to either WT cells or 3 \times FLAG-expressing WT cells. (G) Essentially as in (C) but showing that expressing 3 \times FLAG-TSN in TSN KO#1 cells rescues the levels of CDK2, CCND1, E2F1 and E2F2 mRNAs compared to either WT cells or 3 \times FLAG-expressing WT cells. (H) Histogram representation of RT-qPCR results showing that the level of pri-miR-17-92 is downregulated in TSN KO#1 cells compared to WT cells. All results derive from ≥ 3 independent experiments. Histograms represent the average and SD. * $P < 0.05$, ** $P < 0.01$.

Table S1. Western blot information for experiments involving IP

Figure	Cell equivalents (-IP/+IP)	Antibodies used for Western blots
Fig. 1A	1 : 19.2	α -TSN
	1 : 192	Others
Fig. S1	1 : 5.3	α -FLAG, α -AGO2
	1 : 106	Others

Table S2. Summary of miR-seq data

Sample		Total raw reads	Total reads with inserts between 18-25 nt	Reads mapped to mature miRNAs	Reads mapped to miRs* (the less-abundant strand)	miRNA coverage of mapped reads	miRNA coverage of inserts
Run #1	Ctl siRNA 1	25,579,896	3,296,067	246,216	1,610	95.1	1273.6
	Ctl siRNA 2	32,120,329	4,143,389	270,149	1,772	104.4	1601.0
	Ctl siRNA 3	25,333,117	3,041,702	222,348	1,423	85.9	1175.3
	TSN siRNA 1	34,967,248	7,014,720	1,092,893	7,062	422.3	2710.5
	TSN siRNA 2	25,178,394	5,284,192	796,328	4,962	307.7	2041.8
	TSN siRNA 3	25,740,867	5,194,159	658,619	4,030	254.5	2007.0
Run #2	Ctl siRNA 1	28,025,774	7,426,194	927,532	7,902	358.4	2869.5
	Ctl siRNA 2	36,628,801	12,899,571	1,652,435	15,295	638.5	4984.4
	Ctl siRNA 3	32,658,561	8,689,847	1,115,776	9,717	431.1	3357.7
	TSN siRNA 1	35,311,729	15,822,806	3,140,827	30,963	1213.6	6113.9
	TSN siRNA 2	31,635,725	15,166,522	2,839,173	27,376	1097.1	5860.3
	TSN siRNA 3	32,831,060	8,472,098	1,710,517	14,722	660.9	3273.6

Table S3. Differentially expressed (adjusted *P-value* <0.05) miRNAs upon TSN knockdown in HEK293T cells. Data are derived from two independent miR-seq Runs

ID	<i>P</i> adj* (Run #1)	log2 fold-change upon TSN KD** (Run #1)	<i>P</i> adj (Run #2)	log2 fold-change upon TSN KD** (Run #2)
hsa-miR-4454	8.70E-43	-1.62	2.55E-01	-0.18
hsa-let-7f-5p	2.22E-36	1.02	2.75E-14	0.52
hsa-miR-501-3p	9.02E-33	1.29	1.92E-08	0.65
hsa-miR-99b-5p	2.33E-24	1.21	2.70E-12	0.46
hsa-miR-221-3p	6.13E-22	1.01	3.90E-23	0.73
hsa-miR-125a-5p	1.48E-21	1.21	1.53E-06	0.40
hsa-let-7g-5p	1.60E-18	1.03	1.35E-07	0.38
hsa-miR-378a-3p	1.60E-18	0.69	6.93E-82	1.05
hsa-miR-362-5p	8.93E-16	1.58	2.48E-02	0.76
hsa-miR-375	2.93E-15	1.27	3.58E-53	1.46
hsa-miR-342-3p	2.93E-15	1.19	4.36E-03	0.73
hsa-miR-93-5p	2.20E-13	0.88	9.08E-09	0.41
hsa-miR-182-5p	6.22E-13	0.70	2.25E-03	0.23
hsa-miR-126-5p	8.53E-12	1.15	1.59E-36	1.10
hsa-miR-10b-5p	1.55E-11	0.40	3.43E-01	-0.10
hsa-miR-629-5p	1.78E-11	-1.66	1.23E-16	-1.29
hsa-let-7a-5p	3.64E-11	0.65	1.55E-04	0.25
hsa-miR-16-2-3p	6.20E-11	-2.75	1.02E-41	-2.55
hsa-miR-183-5p	2.08E-10	0.56	9.27E-11	0.46
hsa-miR-1291	2.08E-10	-1.88	NA	0.75
hsa-miR-19a-3p	2.50E-10	0.85	6.60E-03	0.35
hsa-miR-30a-3p	8.46E-09	-0.82	2.55E-09	-0.56
hsa-miR-3960	1.15E-08	-2.77	6.46E-04	-0.96
hsa-miR-532-5p	2.15E-08	0.70	4.07E-28	0.90
hsa-miR-320a	7.08E-08	0.96	1.60E-11	0.58
hsa-miR-19b-3p	1.13E-07	0.79	1.40E-03	0.35
hsa-miR-126-3p	1.62E-07	1.63	1.45E-09	1.11
hsa-miR-1260b	2.04E-07	-1.56	3.29E-01	-0.18
hsa-miR-17-5p	2.34E-07	1.22	2.09E-18	0.62
hsa-miR-98-5p	2.77E-07	1.21	1.10E-07	0.49
hsa-miR-1-3p	3.30E-07	2.81	NA	0.42
hsa-miR-1260a	4.67E-07	-1.66	4.45E-03	-0.45
hsa-miR-92b-3p	1.01E-06	0.64	2.00E-25	0.68
hsa-miR-20a-5p	1.24E-06	1.00	6.11E-02	0.18
hsa-miR-4634	1.36E-06	-1.46	3.70E-31	-1.26
hsa-miR-502-3p	1.52E-06	0.80	3.99E-01	0.22
hsa-miR-30e-3p	4.99E-06	-0.54	4.99E-09	-0.43
hsa-miR-103b	5.50E-06	0.58	1.31E-02	0.19
hsa-miR-103a-3p	8.79E-06	0.58	2.01E-02	0.19
hsa-miR-125b-5p	8.79E-06	-0.73	1.68E-07	-0.85

hsa-miR-9-3p	8.79E-06	1.27	1.31E-01	0.97
hsa-miR-619-5p	8.79E-06	-1.55	4.31E-01	0.34
hsa-miR-152-3p	1.16E-05	-0.84	NA	0.73
hsa-miR-4488	1.81E-05	-1.95	NA	-0.06
hsa-miR-92a-3p	3.96E-05	0.31	1.68E-09	0.39
hsa-miR-148a-5p	4.20E-05	-0.82	7.25E-07	-0.39
hsa-miR-500a-3p	4.20E-05	0.56	6.32E-02	0.28
hsa-miR-4485-3p	5.16E-05	-1.38	3.13E-04	-0.99
hsa-miR-192-5p	0.000116	-0.76	4.59E-15	-0.51
hsa-miR-191-5p	0.000147	0.55	3.99E-01	0.07
hsa-miR-1273g-3p	0.000199	-1.53	1.14E-06	-0.89
hsa-miR-96-5p	0.000206	0.56	2.38E-02	0.52
hsa-miR-1248	0.000231	-1.62	7.42E-04	-1.62
hsa-miR-106b-3p	0.000234	0.65	4.76E-12	0.86
hsa-miR-18a-5p	0.000236	1.03	6.73E-11	0.67
hsa-miR-423-3p	0.000499	0.57	1.86E-01	0.11
hsa-miR-9-5p	0.000599	0.50	5.37E-01	0.07
hsa-miR-10a-3p	0.000721	-0.79	1.15E-12	-0.78
hsa-miR-92a-1-5p	0.000886	-0.70	1.98E-05	-0.50
hsa-miR-340-5p	0.000935	0.57	6.28E-09	0.37
hsa-miR-6087	0.000953	-2.35	1.11E-02	-0.88
hsa-miR-181d-5p	0.000956	0.86	1.52E-15	0.71
hsa-miR-181a-3p	0.001062	-1.49	7.27E-19	-0.82
hsa-miR-7706	0.001361	0.67	8.26E-02	0.17
hsa-let-7i-5p	0.001416	0.81	2.25E-03	0.38
hsa-miR-7641	0.001935	-2.25	NA	-0.24
hsa-miR-1180-3p	0.002889	1.07	2.86E-01	0.11
hsa-miR-550a-5p	0.003161	-1.26	5.60E-03	-0.57
hsa-miR-615-3p	0.003270	-1.13	1.64E-04	-0.37
hsa-miR-3651	0.003309	-1.66	8.00E-01	-0.16
hsa-miR-3648	0.003433	-1.78	NA	-0.35
hsa-miR-25-5p	0.004227	-1.77	4.62E-10	-1.47
hsa-miR-582-3p	0.005223	-0.75	3.70E-09	-0.76
hsa-miR-3130-3p	0.006266	-1.89	NA	-0.96
hsa-miR-663a	0.007952	-1.88	NA	-1.37
hsa-miR-4661-5p	0.008162	-1.54	3.11E-05	-1.10
hsa-miR-660-5p	0.009855	1.07	4.97E-15	0.81
hsa-miR-3529-3p	0.011040	0.42	1.68E-07	-0.56
hsa-miR-708-5p	0.015331	1.26	1.41E-03	0.90
hsa-miR-374b-5p	0.015331	-0.73	2.04E-01	0.40
hsa-miR-455-5p	0.021422	1.32	3.12E-06	1.06
hsa-miR-5096	0.022217	-1.39	1.39E-01	-1.00
hsa-miR-22-3p	0.024730	-1.26	3.37E-17	-0.50
hsa-miR-1271-5p	0.024730	0.23	6.79E-01	0.06
hsa-miR-7-1-3p	0.031168	-1.07	2.53E-04	-0.79

hsa-miR-1268b	0.041456	-1.71	1.24E-03	-0.96
hsa-miR-95-3p	0.049740	0.96	4.62E-01	0.41
hsa-miR-181b-3p	0.061810	-1.51	9.22E-03	-1.14
hsa-miR-204-5p	0.061810	-1.75	7.90E-05	-1.10
hsa-miR-486-5p	0.067198	0.35	9.77E-05	0.28
hsa-miR-361-5p	0.073346	0.37	3.52E-02	0.24
hsa-miR-30c-2-3p	0.073532	-0.89	4.23E-04	-0.78
hsa-miR-671-3p	0.074646	-1.23	2.53E-04	-0.42
hsa-miR-25-3p	0.076565	0.16	4.15E-09	0.33
hsa-miR-26a-5p	0.096990	0.22	5.15E-04	0.21
hsa-miR-26b-5p	0.097511	0.61	6.82E-05	0.49
hsa-miR-195-3p	0.098772	-1.56	2.78E-17	-2.26
hsa-miR-107	0.104465	0.97	8.82E-04	0.31
hsa-miR-320b	0.122525	1.39	1.55E-04	1.25
hsa-let-7c-5p	0.125164	-0.38	4.97E-13	-0.69
hsa-miR-151a-3p	0.132590	0.18	3.40E-07	0.41
hsa-miR-708-3p	0.136442	-1.28	2.59E-02	0.80
hsa-miR-18a-3p	0.146676	1.44	1.22E-03	0.47
hsa-miR-130b-3p	0.179653	0.52	1.79E-28	0.86
hsa-miR-1307-3p	0.185822	0.60	2.19E-17	0.99
hsa-miR-10a-5p	0.214553	-0.12	7.68E-10	-0.49
hsa-miR-151a-5p	0.217412	0.25	6.01E-16	0.59
hsa-miR-181b-5p	0.242887	-0.23	5.01E-08	-0.38
hsa-miR-99a-5p	0.255986	-0.20	6.17E-09	-0.61
hsa-miR-378a-5p	0.259035	0.68	7.06E-05	0.92
hsa-miR-34a-5p	0.261143	0.83	2.64E-05	0.71
hsa-miR-1303	0.261143	-0.85	1.06E-07	-1.07
hsa-miR-625-3p	0.267020	-0.89	2.36E-03	-0.94
hsa-miR-7974	0.292964	-0.36	1.71E-41	-0.99
hsa-miR-503-5p	0.306860	0.28	4.38E-02	0.99
hsa-let-7e-5p	0.333966	0.28	9.35E-11	0.53
hsa-miR-28-3p	0.351138	-0.13	9.71E-03	-0.18
hsa-miR-27b-3p	0.371827	-0.21	7.97E-08	0.38
hsa-miR-1285-3p	0.378316	-0.79	8.44E-15	-0.88
hsa-miR-1269b	0.398792	-0.18	5.31E-03	-0.33
hsa-miR-582-5p	0.406022	-0.64	1.16E-06	-1.26
hsa-miR-106b-5p	0.435738	0.30	3.83E-09	0.82
hsa-miR-5701	0.435738	-0.97	1.49E-02	-0.39
hsa-miR-222-3p	0.454404	0.15	2.01E-10	0.70
hsa-miR-27b-5p	0.469184	-0.60	9.37E-03	-0.53
hsa-miR-455-3p	0.469184	0.45	1.03E-02	1.62
hsa-miR-186-5p	0.511417	0.16	1.29E-04	0.23
hsa-miR-339-5p	0.532518	0.40	6.42E-04	0.64
hsa-miR-125b-2-3p	0.536720	-0.65	3.24E-19	-1.61
hsa-miR-629-3p	0.562418	-0.52	6.23E-12	-2.09

hsa-miR-561-5p	0.582495	-0.64	1.76E-08	-0.68
hsa-miR-484	0.599576	0.14	7.40E-05	0.34
hsa-miR-222-5p	0.622585	0.29	2.51E-06	0.88
hsa-miR-589-5p	0.629437	0.09	2.36E-03	0.30
hsa-miR-130b-5p	0.652040	-0.30	1.25E-02	0.83
hsa-miR-21-5p	0.661200	0.13	3.13E-04	0.31
hsa-miR-30e-5p	0.661200	-0.34	4.71E-02	0.47
hsa-miR-181a-5p	0.714801	-0.12	2.88E-02	-0.14
hsa-miR-4677-3p	0.760971	-0.16	1.51E-04	-0.52
hsa-miR-17-3p	0.778057	0.11	3.12E-06	0.78
hsa-miR-378c	0.802746	0.20	1.34E-14	1.13
hsa-miR-1307-5p	0.850716	-0.25	3.53E-13	0.68
hsa-miR-652-3p	0.856199	0.08	1.11E-02	0.67
hsa-miR-140-3p	0.859165	0.11	4.41E-03	0.92
hsa-miR-101-3p	0.864258	-0.07	2.11E-06	0.63
hsa-miR-424-5p	0.864258	-0.15	1.57E-03	0.56
hsa-miR-128-3p	0.866793	0.03	2.20E-06	0.43
hsa-miR-187-3p	0.891954	-0.17	5.30E-03	0.59
hsa-miR-27a-3p	0.894721	-0.12	4.02E-05	0.65
hsa-miR-3662	0.894721	0.13	9.22E-03	-1.13
hsa-miR-148b-3p	0.929791	-0.02	1.99E-03	0.31
hsa-miR-641	0.946770	0.07	1.87E-10	-0.85
hsa-miR-548k	0.946770	-0.06	8.19E-09	-0.54
hsa-miR-3184-5p	0.946770	0.04	1.40E-08	0.75
hsa-miR-15a-5p	0.998843	0.00	5.70E-06	0.41
hsa-miR-21-3p	NA	0.37	1.34E-08	-0.64
hsa-miR-32-5p	NA	0.66	2.31E-03	0.73
hsa-miR-181c-5p	NA	-0.45	7.57E-17	0.93
hsa-miR-196a-3p	NA	-0.65	3.26E-03	-1.25
hsa-miR-30b-3p	NA	-0.13	4.26E-02	-0.71
hsa-miR-30c-1-3p	NA	-1.66	7.43E-05	-0.77
hsa-miR-34c-5p	NA	NA	4.23E-04	1.61
hsa-miR-365a-5p	NA	0.20	2.48E-02	-1.42
hsa-miR-365a-3p	NA	1.12	2.09E-02	0.81
hsa-miR-324-3p	NA	-0.50	3.04E-02	0.99
hsa-miR-449a	NA	-1.09	9.22E-03	-0.82
hsa-miR-550a-3p	NA	-0.68	4.79E-04	-0.87
hsa-miR-615-5p	NA	0.24	7.25E-04	-1.07
hsa-miR-33b-5p	NA	0.18	1.36E-05	1.63
hsa-miR-378d	NA	1.17	8.44E-03	1.20
hsa-miR-874-5p	NA	1.32	4.91E-02	-0.94
hsa-miR-548f-5p	NA	-0.07	1.26E-04	-0.84
hsa-miR-548g-3p	NA	1.71	3.78E-04	1.35
hsa-miR-1266-5p	NA	0.36	5.62E-03	-0.99
hsa-miR-1910-5p	NA	-0.96	1.07E-02	0.65

hsa-miR-3158-3p	NA	-0.91	8.29E-05	-0.59
hsa-miR-3607-3p	NA	0.12	2.75E-03	-0.66
hsa-miR-3615	NA	-0.22	2.69E-02	0.83
hsa-miR-3688-3p	NA	-0.59	7.37E-03	-1.65
hsa-miR-550b-2-5p	NA	-0.72	3.42E-04	-0.85
hsa-miR-4661-3p	NA	-2.10	7.62E-05	-1.76
hsa-miR-4787-3p	NA	0.50	1.39E-03	1.06

*Adjusted *P*-value

**Knockdown

Table S4. List of significantly upregulated (adjusted P -value <0.05) miRNAs that are in common to both Run #1 and Run #2 miR-seq experiments

ID	P_{adj}^* (Run #1)	log2 fold-change upon TSN KD** (Run #1)	P_{adj}^* (Run #2)	log2 fold-change upon TSN KD** (Run #2)
hsa-miR-126-3p	1.62.E-07	1.63	1.45.E-09	1.11
hsa-miR-362-5p	8.93.E-16	1.58	2.48.E-02	0.76
hsa-miR-455-5p	2.14.E-02	1.32	3.12.E-06	1.06
hsa-miR-501-3p	9.02.E-33	1.29	1.92.E-08	0.65
hsa-miR-375	2.93.E-15	1.27	3.58.E-53	1.46
hsa-miR-708-5p	1.53.E-02	1.26	1.41.E-03	0.90
hsa-miR-17-5p	2.34.E-07	1.22	2.09.E-18	0.62
hsa-miR-125a-5p	1.48.E-21	1.21	1.53.E-06	0.40
hsa-miR-98-5p	2.77.E-07	1.21	1.10.E-07	0.49
hsa-miR-99b-5p	2.33.E-24	1.21	2.70.E-12	0.46
hsa-miR-342-3p	2.93.E-15	1.19	4.36.E-03	0.73
hsa-miR-126-5p	8.53.E-12	1.15	1.59.E-36	1.10
hsa-miR-660-5p	9.86.E-03	1.07	4.97.E-15	0.81
hsa-miR-18a-5p	2.36.E-04	1.03	6.73.E-11	0.67
hsa-let-7g-5p	1.60.E-18	1.03	1.35.E-07	0.38
hsa-let-7f-5p	2.22.E-36	1.02	2.75.E-14	0.52
hsa-miR-221-3p	6.13.E-22	1.01	3.90.E-23	0.73
hsa-miR-320a	7.08.E-08	0.96	1.60.E-11	0.58
hsa-miR-93-5p	2.20.E-13	0.88	9.08.E-09	0.41
hsa-miR-181d-5p	9.56.E-04	0.86	1.52.E-15	0.71
hsa-miR-19a-3p	2.50.E-10	0.85	6.60.E-03	0.35
hsa-let-7i-5p	1.42.E-03	0.81	2.25.E-03	0.38
hsa-miR-19b-3p	1.13.E-07	0.79	1.40.E-03	0.35
hsa-miR-532-5p	2.15.E-08	0.70	4.07.E-28	0.90
hsa-miR-182-5p	6.22.E-13	0.70	2.25.E-03	0.23
hsa-miR-378a-3p	1.60.E-18	0.69	6.93.E-82	1.05
hsa-let-7a-5p	3.64.E-11	0.65	1.55.E-04	0.25
hsa-miR-106b-3p	2.34.E-04	0.65	4.76.E-12	0.86
hsa-miR-92b-3p	1.01.E-06	0.64	2.00.E-25	0.68
hsa-miR-103a-3p	8.79.E-06	0.58	2.01.E-02	0.19
hsa-miR-103b	5.50.E-06	0.58	1.31.E-02	0.19
hsa-miR-340-5p	9.35.E-04	0.57	6.28.E-09	0.37
hsa-miR-96-5p	2.06.E-04	0.56	2.38.E-02	0.52
hsa-miR-183-5p	2.08.E-10	0.56	9.27.E-11	0.46
hsa-miR-92a-3p	3.96.E-05	0.31	1.68.E-09	0.39

*Adjusted P -value

**Knockdown

Table S5. Sequences of putative human TumorID targets and their orthologs in mouse, all of which are predicted to also be TumorID targets

Human				Mouse					
ID	Accession number	Sequence	Position of U/A	Position of C/A	ID	Accession number	Sequence	Position of U/A	Position of C/A
hsa-miR-126-3p	MIMAT0000445	UCG UA CCGUAGU AA U UA UCCG	4, 13, 16	—	mmu-miR-126a-3p	MIMAT0000138	UCG UA CCGUAGU UA UAUGCG	4, 13, 16	—
hsa-miR-362-5p	MIMAT0000705	AAUCUUUGAA CCUA GGUUGAGU	14	—	mmu-miR-362-5p	MIMAT0000706	AAUCCUUUGAA CCUA GGUUGAGUAU	14	—
hsa-miR-455-5p	MIMAT0003150	UA UUGUCCUUUGAG CAUA UCCG	1, 16	18	mmu-miR-455-5p	MIMAT0003485	UA UUGUCCUUUGAG CAUA UCCG	1, 16	18
hsa-miR-501-3p	MIMAT0004774	AAUG CA CCCGGG CA AGGAUUUC	5, 13	—	mmu-miR-501-3p	MIMAT0003509	AAUG CA CCCGGG CA AGGAUUUC	—	5, 13
hsa-miR-375	MIMAT0000728	UUUGUUCCUUCGGCCGCGGUA	—	—	mmu-miR-375-3p	MIMAT0000739	UUUGUUCGUUCGGCCGCGGUA	—	—
hsa-miR-708-5p	MIMAT0004926	AAAGAGCU UA CA AUCUA GGUGGG	9, 16	11,	mmu-miR-708-5p	MIMAT0000428	AAAGAGCU UA CA AUCUA GGUGGG	9, 16	11
hsa-miR-17-5p	MIMAT0000070	CA AAAGUCCU UA CA GU CG CA GGUAG	10, 21	1, 12, 17	mmu-miR-17-5p	MIMAT0000649	CA AAAGUCCU UA CA GU CG CA GGUAG	10, 21	1, 12, 17
hsa-miR-125a-5p	MIMAT0000443	UCCCGAGAGACCCUU UA ACCUGUA	15	—	mmu-miR-125a-5p	MIMAT0000135	UCCCGAGAGACCCUU UA ACCUGUA	15	—
hsa-miR-98-5p	MIMAT0000096	UGAGG UA GU UA AGUUUG UA UUUGU	6, 9, 16	—	mmu-miR-98-5p	MIMAT0000545	UGAGG UA GU UA AGUUUG UA UUUGU	6, 9, 16	—
hsa-miR-99b-5p	MIMAT0000689	CA CCCG UA GA ACC GA CC UUUGC	7	1	mmu-miR-99b-5p	MIMAT0000132	CA CCCG UA GA ACC GA CC UUUGC	7	1
hsa-miR-342-3p	MIMAT0000753	UCU CA CA CA GA AA AU CG CA CC CGU	—	4, 6, 8, 17	mmu-miR-342-3p	MIMAT0000590	UCU CA CA CA GA AA AU CG CA CC CGU	—	4, 6, 8, 17
hsa-miR-126-5p	MIMAT0000444	CA UU UA UU UA CUUUUG UA CGCG	4, 7, 16	1	mmu-miR-126a-5p	MIMAT0000137	CA UU UA UU UA CUUUUG UA CGCG	4, 7, 16	1
hsa-miR-660-5p	MIMAT0003338	UA CC CA UU GC CA UA UCCGAGAUUG	1, 12	5, 10	—	—	—	—	—
hsa-miR-18a-5p	MIMAT0000072	UA AGGU GC AU CU GA GU UG UA CA UA U G	1, 12, 21	8, 17	mmu-miR-18a-5p	MIMAT0000528	UA AGGU GC AU CU GA GU UG UA CA UA U G	1, 12, 21	8, 17
hsa-let-7g-5p	MIMAT0000414	UGAGG UA GU UA AGUUUG UA CA GU U	6, 9, 16	18	mmu-let-7g-5p	MIMAT0000121	UGAGG UA GU UA AGUUUG UA CA GU U	6, 9, 16	18
hsa-let-7f-5p	MIMAT0000067	UGAGG UA GU UA AGUUUG UA U UA GUU	6, 9, 16, 18	—	mmu-let-7f-5p	MIMAT0000525	UGAGG UA GU UA AGUUUG UA U UA GUU	6, 9, 16, 18	—
hsa-miR-221-3p	MIMAT0000278	AGCU UA CAUUUGUCUCCUGGCUUUC	4	6	mmu-miR-221-3p	MIMAT0000669	AGCU UA CAUUUGUCUCCUGGCUUUC	4	6
hsa-miR-320a	MIMAT0000510	AAAAGCUGGUGUAGAGGGCGGA	—	—	—	—	—	—	—
hsa-miR-93-5p	MIMAT0000093	CA AAAGUCGUUCGCG CA GGU UG	21	1, 17	mmu-miR-93-5p	MIMAT0000540	CA AAAGUCGUUCGCG CA GGU UG	21	1, 17
hsa-miR-181d-5p	MIMAT0002821	AA CA UU CAUUUGUUUGCCGUGGGU	—	3, 7	mmu-miR-181d-5p	MIMAT0004324	AA CA UU CAUUUGUUUGCCGUGGGU	—	3, 7
hsa-miR-19a-3p	MIMAT0000073	UGUG CA AAU CU U GC AAAACU GA	11	5, 15	mmu-miR-19a-3p	MIMAT0000651	UGUG CA AAU CU U GC AAAACU GA	11	5, 15
hsa-let-7i-5p	MIMAT0000415	UGAGG UA GU UA AGUUUGGCUUUU	6, 9	—	mmu-let-7i-5p	MIMAT0000122	UGAGG UA GU UA AGUUUGGCUUUU	6, 9	—
hsa-miR-19b-3p	MIMAT0000074	UGUG CA AAU CU U GC AAAACU GA	—	5, 11, 15	mmu-miR-19b-3p	MIMAT0000513	UGUG CA AAU CU U GC AAAACU GA	—	5, 11, 15
hsa-miR-532-5p	MIMAT0002888	CA UUGCCUUGAGUG UA GGACCGU	14	1	mmu-miR-532-5p	MIMAT0002889	CA UUGCCUUGAGUG UA GGACCGU	14	1
hsa-miR-182-5p	MIMAT0000259	UUUGG CA AAU GU GA AA CU CA CA CU	12	6, 19, 21	mmu-miR-182-5p	MIMAT0000211	UUUGG CA AAU GU GA AA CU CA CA CU	12	6, 19, 21
hsa-miR-378a-3p	MIMAT0000732	ACUGGACUU GGAGU CA GA AA GGC	—	15	mmu-miR-378a-3p	MIMAT0003151	ACUGGACUU GGAGU CA GA AA GGC	—	15
hsa-let-7a-5p	MIMAT0000062	UGAGG UA GU UA AGUUUG UA U UA GUU	6, 9, 16, 18	—	mmu-let-7a-5p	MIMAT0000521	UGAGG UA GU UA AGUUUG UA U UA GUU	6, 9, 16, 18	—
hsa-miR-106b-3p	MIMAT0004672	CCG CA CUUGUGG UA CUUGCUGC	13	4	mmu-miR-106b-3p	MIMAT0004582	CCG CA CUUGUGG UA CUUGCUGC	13	4
hsa-miR-92b-3p	MIMAT0003218	UA UUG CA CUUGCUGCCCGGCCUCC	1	6	mmu-miR-92b-3p	MIMAT0004899	UA UUG CA CUUGCUGCCCGGCCUCC	1	6
hsa-miR-103a-3p	MIMAT0000101	AG CA GA CA U GU U GC AGGGC UA UGA	11, 19	3, 6, 13	—	—	—	—	—
hsa-miR-103b	MIMAT0007402	UCA U AG CCCU GU CA UA U GU CGCU	4, 11	2, 13	—	—	—	—	—
hsa-miR-340-5p	MIMAT0004692	UUA U UA AA GC AAU GA GA CU GAUU	2, 4	9	mmu-miR-340-5p	MIMAT0004651	UUA U UA AA GC AAU GA GA CU GAUU	2, 4	9
hsa-miR-96-5p	MIMAT0000095	UUUGG CA CU GA CA CA UUUUUU GU CU	9	6, 12, 14	mmu-miR-96-5p	MIMAT0000541	UUUGG CA CU GA CA CA UUUUUU GU CU	9	6, 12, 14
hsa-miR-183-5p	MIMAT0000261	UA UUG CA CUUG UA GA UU CA CU	1, 12	6, 19	mmu-miR-183-5p	MIMAT0000212	UA UUG CA CUUG UA GA UU CA CU	1, 12	6, 19
hsa-miR-92a-3p	MIMAT0000092	UA UUG CA CUUGCUGCCCGGCCUUG	1	6	mmu-miR-92a-3p	MIMAT0000539	UA UUG CA CUUGCUGCCCGGCCUUG	1	6

Tabulation is limited to human miRNAs that have an identifiable mouse ortholog. CA dinucleotides are shown in red, and UA dinucleotides are shown in blue.

Table S6. DNA oligos used in plasmid constructions

Plasmid name	Template plasmid used to generate 5' and 3' fragments	Sense (S) and antisense (AS) PCR primers used to generate 5' fragment	Sense (S) and antisense (AS) PCR primers used to generate 3' fragment	Restriction enzyme used to digest PCR products and vectors
pET28a-TSN ΔSN2(Δ164-306)	pET28a-TSN (1-885)	S: 5'-GCGGCAGCCATATGGCTAGCATGAC-3' AS: 5'-CAAATTAGCTGTGGGTCCACAAAGTGCCCT-3'	S: 5'-AGGCACTTTGTGACCCCAACAGCTAATTTG-3' AS: 5'-CTTGTAAGCTAGCAGATCGCTCCTTC-3'	NheI
pET28a-TSN ΔSN3(Δ312-467)	pET28a-TSN (1-885)	S: 5'-GCCGGCAGCCATATGGCTAGCATGAC-3' AS: 5'-CTTCTTGCTATGCAACAATTAGCTGTGGG-3'	S: 5'-CCCACAGCTAATTTGTTGCATAGCAAGAAG-3' AS: 5'-CTTGTAAGCTAGCAGATCGCTCCTTC-3'	NheI
pET28a-TSN ΔSN4(Δ500-635)	pET28a-TSN (1-885)	S: 5'-ATCACAGAGCTCCCTCGAAGGAAG-3' AS: 5'-GGGCTGCTCCCAIATIGCCCCGCTGAAGAAAA G-3'	S: 5'-CCCCAAGATGATGATTAAGGAGGATCGG-3' AS: 5'-GTGCTCGAGTGGCGCCGCAAGCTTG-3'	SacI
pCDNA3- 3×FLAG-AGO2 ^R	pCDNA3- 3×FLAG- AGO2	S: 5'-CAAAGGAATTCATGTACTCGGAGGCC-3' AS: 5'-TTTATGCAGCCGCTGGCCGACCACAATGTTAC AGAC-3'	S: 5'-GCCCGGCCAAGCGCTGCAT4AAAAAATTAACGG ACAATC-3' AS: 5'-GCAGAATTCACAAGCAAAAGTACATGGTG-3'	EcoRI

Underlined nucleotides specify restriction enzyme sites; superscript R denotes resistance to AGO2 siRNA; bold and italicized nucleotides specify changes that confer siRNA-resistance.

Table S7. DNA oligos used in constructing sgRNA-expression plasmids

Plasmid name	Sense (S) and antisense (AS) DNA oligos
pSpCas9n(BB)-2A-Puro-TSN-sgRNA2	S: 5'-CACCGGTGCTGGAAATCTTGCTCGC-3' AS: 5'-AAACGCGAGCAAGATTTCCAGCACC-3'
pSpCas9n(BB)-2A-Puro-TSN-sgRNA3	S: 5'-CACCGTCCCAATCAGCTTCTTTCGA-3' AS: 5'-AAACTCGAAAGAAGCTGATTGGGAC-3'
pSpCas9n(BB)-2A-Puro-TSN-sgRNA4	S: 5'-CACCGACTCCCCAGGGGCGAGAGTA-3' AS: 5'-AAACTACTCTCGCCCCTGGGGAGTC-3'

Table S8. Primers used for qPCR quantitation of mRNAs

Figure	Transcript	Sense (S) and antisense (AS) PCR primers	Region spanned by the primer pair
Fig. S19	TSN mRNA	S: 5'-CCTTGAAAAGATAACCAATGG-3'	exon 3–exon 5
		AS: 5'-TCTGCTCAGGATTATTAGCTC-3'	
		S: 5'-GAACACCCAGGATAAGAACA-3'	exon 10–exon 12
	AS: 5'-TCACATTGACCTTCTTCCCA-3'		
	S: 5'-CTACGGCAACAGAGAGGTCC-3'	exon 20–exon 22	
	AS: 5'-GGGCATCATCATCTTGGGGC-3'		
GAPDH mRNA	S: 5'-GTCGCCAGCCGAGCCACATC-3'		
	AS: 5'-CCAGGCGCCCAATACGACCA-3'		